Nanoscale Advances

REVIEW

View Article Online
View Journal | View Issue

Cite this: *Nanoscale Adv.*, 2024, **6**, 5478

Gold on the horizon: unveiling the chemistry, applications and future prospects of 2D monolayers of gold nanoparticles (Au-NPs)

Tholkappiyan Ramachandran, *[a] Ashraf Ali,[a] Haider Butt,[b] Lianxi Zheng,[b] Firdous Ahmad Deader[a] and Moh'd Rezeq*[ac]

Noble 2D monolayers of gold nanoparticles (Au-NPs) have garnered significant attention due to their unique physicochemical properties, which are instrumental in various technological applications. This review delves into the intricate physical chemistry underlying the formation of Au-NP monolayers, highlighting key interactions such as electrostatic forces, van der Waals attractions, and ligand-mediated stabilization. The discussion extends to the size- and shape-dependent assembly processes of these NP monolayers, elucidating how nanoparticle dimensions and morphologies influence monolayer formation and stability. Moreover, the review explores the diverse interfaces—solid, liquid, and air—where Au-NP monolayers are employed, each presenting distinct advantages and challenges. In the realm of applications, Au-NP monolayers have shown remarkable promises. In memory devices, their ability to facilitate high-density data storage through enhanced electron transport mechanisms is examined. Biosensing applications benefit from the monolayers' exceptional sensitivity and specificity, which are crucial for detecting biomolecular interactions. Furthermore, the role of Au-NP monolayers in electrocatalysis is explored, with a focus on their catalytic efficiency and stability in various electrochemical reactions. Despite their potential, the deployment of Au-NP monolayers faces several challenges. The review addresses current limitations such as scalability, reproducibility, and long-term stability, proposing potential strategies to overcome these hurdles. Future prospects are also discussed, including the development of multifunctional monolayers and integration with other nanomaterials to enhance performance across different applications. In conclusion, while significant strides have been made in understanding and utilizing 2D Au-NP monolayers, ongoing research is imperative to fully exploit their capabilities. Addressing existing challenges through innovative approaches will pave the way for their widespread adoption in advanced technological applications.

Received 12th August 2024
Accepted 30th September 2024

DOI: 10.1039/d4na00666f

rsc.li/nanoscale-advances

1. Introduction

Gold nanoparticles (Au-NPs) are highly significant across a spectrum of scientific and technological domains owing to their unique properties and versatile functionalities. Gold Au-NPs offer distinct advantages over bulk gold materials in various applications, making them preferable in many scenarios. One significant advantage of Au-NPs is their high surface area-to-volume ratio, which enhances surface effects such as surface plasmon resonance (SPR) and surface reactivity. This property enables Au-NPs to exhibit tunable optical and electronic properties, making them highly desirable for sensing, imaging, and optoelectronics applications. Gold nanoparticle assemblies encompass a diverse array of structures, each with unique properties and applications. Linear assemblies, formed through self-assembly processes or templated approaches, consist of gold nanoparticles arranged in a one-dimensional configuration, exhibiting distinct optical and electronic properties due to plasmon coupling between adjacent nanoparticles.[1] Two-dimensional monolayer films, densely packed on a substrate surface, offer precise control over interparticle spacing and interaction, facilitating tunable properties such as enhanced catalytic activity and optical response.[2] Three-dimensional superstructures, including clusters and hierarchical architectures, are constructed through controlled aggregation or template-directed synthesis, offering enhanced plasmonic coupling and mechanical strength.[3] Core–shell structures, where gold nanoparticles are coated or encapsulated with another material, combine the unique properties of gold with the functional attributes of the

[a]*Department of Physics, Khalifa University of Science and Technology, Abu Dhabi, P. O. Box 127788, United Arab Emirates. E-mail: tholkappiyan.ramachandran@ku.ac.ae; mohd.rezeq@ku.ac.ae*

[b]*Department of Mechanical & Nuclear Engineering, Khalifa University of Science and Technology, Abu Dhabi, P. O. Box 127788, United Arab Emirates*

[c]*System on Chip Lab (SoCL), Khalifa University of Science and Technology, Abu Dhabi, P. O. Box 127788, United Arab Emirates*

surrounding shell material, enhancing stability and biocompatibility for biomedical applications.[4] Additionally, hybrid nanocomposites incorporate gold nanoparticles into matrices composed of polymers, ceramics, or carbon-based materials, offering versatility and synergistic effects for applications in catalysis, electronics, and energy storage. These diverse assembly types serve as valuable building blocks for a wide range of applications in science and technology, showcasing the versatility and potential of gold nanoparticles in various fields.

Recent advancements in assembly approaches for gold nanoparticles have focused on achieving precise control over assembly structures, enhancing scalability, and enabling novel functionalities.[5] DNA-mediated assembly techniques utilize complementary DNA strands attached to gold nanoparticles to programmable control their assembly into specific structures, such as DNA origami templates and DNA-based scaffolds. Directed self-assembly methods leverage external fields, like electric or magnetic fields, to guide the assembly of gold nanoparticles into desired configurations, such as ordered arrays, rings, and lattices. Microfluidic-based assembly approaches offer precise control over fluid flow and mixing at the microscale, enabling the rapid and scalable fabrication of gold nanoparticle assemblies, including hierarchical structures and functionalized patterns. Templated assembly techniques utilize pre-patterned substrates or templates to guide the arrangement of gold nanoparticles into specific geometries, such as nanopatterned surfaces and biomolecular scaffolds. Dynamic assembly approaches involve reversible and programmable assembly of gold nanoparticles driven by external stimuli, such as pH, temperature, or light, enabling dynamic control over assembly and disassembly for applications in drug delivery, sensing, and nanomachines. These recent assembly strategies demonstrate the diverse and innovative approaches being pursued to advance the field of gold nanoparticle assembly, offering new opportunities for tailoring nanoparticle properties and functionalities for various applications.

Monolayer Au-NPs offer a plethora of benefits derived from their unique properties, including high surface-to-volume ratio, plasmonic, and biocompatibility, rendering them highly coveted for a wide range of applications like catalysts, surface-enhanced spectroscopy, photothermal therapy, and optical sensing, drug delivery, imaging, and therapeutics. Monolayer Au-NPs can be assembled into diverse configurations, including 2D monolayer films, nanocomposites, and hierarchical structures, offering tailored materials with specific properties and functionalities for applications in electronics, photonics, and energy storage. Across various fields, monolayer Au-NPs find applications in drug delivery systems, biosensors, imaging contrast agents, therapeutic agents for cancer treatment and diagnostics, catalysis for organic synthesis and energy conversion, biosensors for biomolecule detection, and photonic devices for telecommunications and data storage. Furthermore, their versatility extends to environmental applications such as pollutant detection and remediation, highlighting their potential to address pressing challenges in sustainability and environmental protection. The multifaceted utility of monolayer Au-NPs underscores their indispensable role in modern materials science, nanotechnology, biomedicine, and environmental science, driving innovation and advancement in diverse scientific and technological domains.

Fig. 1 shows the data from Web of Science regarding the distribution of research on monolayers of gold nanoparticles across different countries and regions, revealing a diverse global landscape of scientific inquiry. Notably, the United States emerges as a significant contributor, with 2596 records, constituting the largest share at 24.945%. Following closely behind is China, with 2133 records, accounting for 20.496% of the total publications. These two countries together represent a substantial portion of the research output in this field. Other notable contributors include People's Republic of Japan, with a significant 818 records (7.86%), and Germany, with 713 records (6.851%). These findings suggest a widespread interest in and engagement with the topic across various continents and regions. Furthermore, while some countries exhibit relatively lower publication counts individually, their collective contributions underscore the global collaboration and exchange of knowledge in advancing the understanding and applications of monolayers of gold nanoparticles. This global distribution reflects the interdisciplinary nature of research, with contributions from diverse scientific communities around the world.

Fig. 2 shows the data from Web of Science indicates a consistent interest in monolayers of gold nanoparticles over the years, with a notable increase in research activity in recent times. In the final publication year of 2024, there were 91 records, comprising 0.874% of the total 10 407 publications. While this constitutes a relatively small percentage, it reflects ongoing interest and exploration in this field. Looking back, there has been a steady growth in research output since the mid-1990s, with occasional fluctuations but an overall upward trajectory. Notably, from 2010 onwards, there has been a consistent rise in publications, peaking in 2011 with 626 records. This suggests a sustained interest and possibly advancements in understanding or applications of monolayers of gold nanoparticles during this period. The data underscores the enduring significance of this area of study within the scientific community, likely driven by its potential in various fields such as nanotechnology, materials science, and biomedical applications.

This review article aims to delve comprehensively into the multifaceted realm of two-dimensional (2D) monolayers of Au-NPs, with a focus on elucidating their formation mechanisms, unique physicochemical properties, and diverse applications across different interfaces. By synthesizing recent research findings and insights, the objective is to provide a thorough understanding of the intricate physics and chemistry underlying the assembly and stabilization of Au-NP monolayers. Special emphasis is placed on exploring key interactions such as electrostatic forces, van der Waals attractions, and ligand-mediated stabilization, and how these interactions influence the size- and shape-dependent assembly processes. Furthermore, the review seeks to examine the performance of Au-NP monolayers in various technological applications, including but not limited to memory devices, biosensing, and

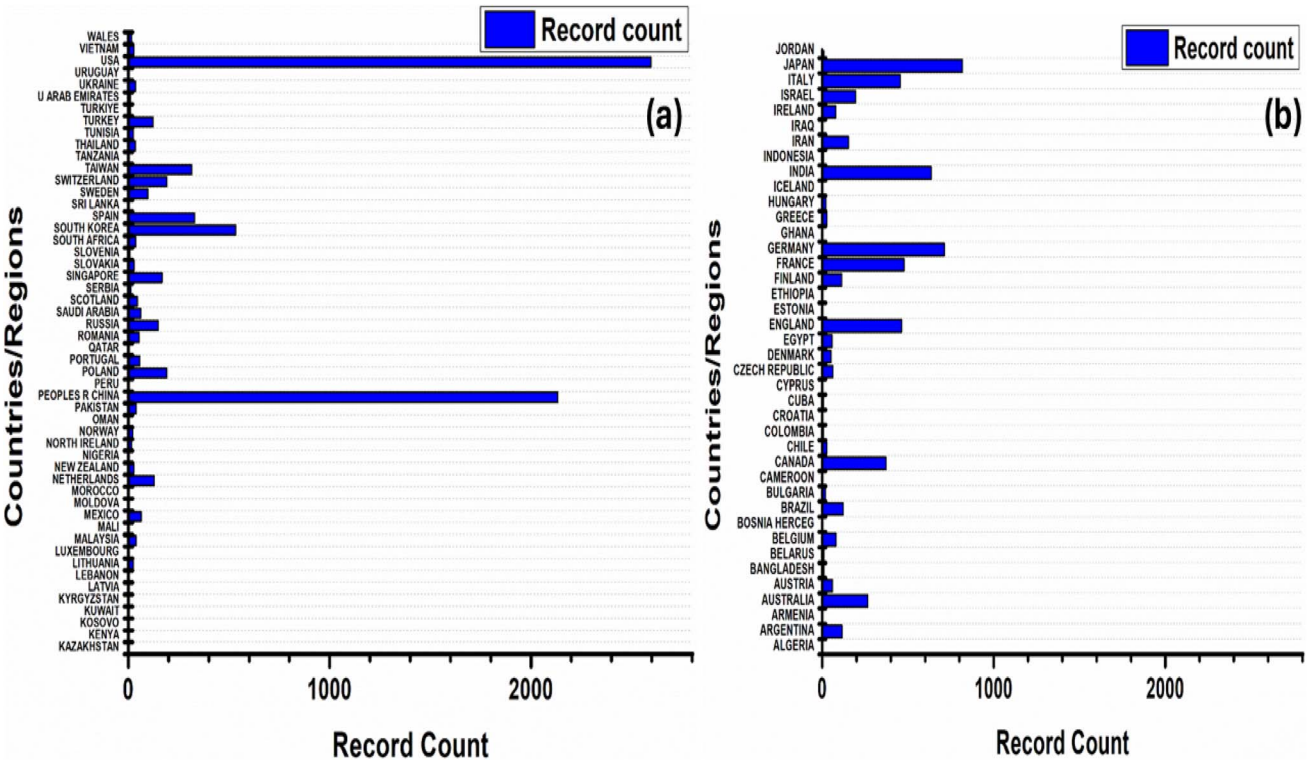

Fig. 1 Global distribution of research on monolayers of gold nanoparticles: (a and b) country-wise contribution when searched with keyword "monolayers of gold nanoparticles (Topic)" [Web of Science].

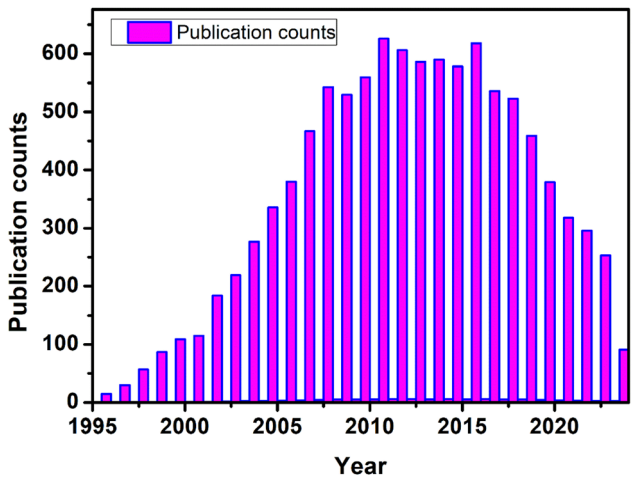

Fig. 2 Impression of the research contributions related to monolayer Au-NPs when searched with keyword "monolayers of gold nanoparticles (Topic)" [Web of Science].

electrocatalysis. Specifically, it aims to elucidate how the unique properties of Au-NP monolayers, such as their high electron transport efficiency, exceptional sensitivity, and catalytic activity, contribute to enhancing device performance and functionality in these applications. In addition to highlighting the potential of Au-NP monolayers, the review also addresses the current challenges hindering their widespread deployment. These challenges encompass issues related to scalability, reproducibility, and long-term stability, which are crucial for practical applications. To tackle these challenges, potential strategies and future prospects are discussed, including advancements in synthesis techniques, surface engineering approaches, and integration with other nanomaterials to develop multifunctional monolayers with enhanced performance characteristics. In conclusion, this review underscores the significant strides made in understanding and harnessing the capabilities of 2D Au-NP monolayers, while also emphasizing the importance of ongoing research to fully exploit their potential. By identifying current challenges and proposing innovative solutions, the review aims to catalyze further advancements in the field and pave the way for the widespread adoption of Au-NP monolayers in advanced technological applications.

2. Key aspects of the chemistry behind the Au-NPs monolayer

Understanding the key aspects of the physical chemistry governing the formation of these films is essential for harnessing their full potential in various fields. At the heart of the chemistry behind the formation of 2D Au-NP monolayer films lies the self-assembly process. Self-assembly is a spontaneous and highly organized process driven by the interactions between individual nanoparticles. In the case of Au-NPs, self-assembly occurs on a substrate surface and is mediated by a combination of intermolecular forces, including electrostatic interactions, van der

Waals forces, and ligand-mediated interactions. These forces orchestrate the arrangement of Au-NPs into ordered arrays, ultimately dictating the structure and properties of the resulting monolayer films.

2.1. Electrostatic interactions

The physical chemistry underlying the formation of 2D monolayer films of Au-NPs through electrostatic interactions is a burgeoning field with significant implications for various applications. Electrostatic forces, a fundamental aspect of colloidal science, play a pivotal role in guiding the assembly of Au-NPs on substrates. This assembly process relies on the interaction between charged species present on the surface of the Au-NPs and those on the substrate. The charged entities can originate from capping ligands on the nanoparticles or functional groups on the substrate surface. When these charged entities have opposite charges, electrostatic attraction drives the assembly of the Au-NPs into well-defined monolayer films. The mechanism of assembly *via* electrostatic interactions involves several key steps. Initially, the substrate surface is modified to carry a specific charge, either positive or negative, depending on the desired assembly configuration. This modification can be achieved through functionalization with charged molecules to induce surface charging. Subsequently, Au-NPs capped with ligands bearing complementary charges are introduced into the system. The electrostatic attraction between the charged ligands on the Au-NPs and the oppositely charged surface facilitates the adsorption and self-assembly of the nanoparticles onto the substrate. It is reported from C. Burns *et al.*[5] reported an intriguing phenomenon during their routine investigation of surface-modified Au-NPs. They observed that this finding aligns with the understanding that surface charge, arising from adsorbed species on the Au-NPs surface, significantly affects the stability of the nanoparticle solution and the mean distance between particles during Brownian motion. Since ionic strength directly influences the Debye length surrounding the particles, it was hypothesized that variations in ionic strength could alter the mean closest approach distance between Au-NPs. By controlling the ionic strength, it is therefore possible to fine-tune the mean encounter distance between the nanoparticles, potentially offering a method to regulate their interactions and assembly in solution.

In the literature, numerous studies have demonstrated the versatility and controllability of electrostatic-driven assembly approaches for fabricating 2D Au-NP monolayer films. For example, Smith *et al.* (2018)[6] explored the assembly of Au-NPs on positively charged surfaces, leveraging electrostatic interactions to achieve highly ordered arrays. By tuning the surface charge density and the concentration of Au-NPs, they demonstrated precise control over the packing density and morphology of the monolayer films. Similarly, Chen *et al.* (2021)[7] investigated the assembly of Au-NPs on negatively charged substrates, highlighting the role of electrostatic interactions in dictating nanoparticle organization. Further insights into the mechanism of electrostatic-driven assembly have been gained through theoretical modeling and computational simulations. These studies have elucidated the interplay between electrostatic forces, steric effects, and solvent interactions, providing a comprehensive understanding of the factors governing nanoparticle assembly at the molecular level.

By incorporating such insights, researchers can design strategies to optimize the assembly process and tailor the properties of Au-NP monolayer films for specific applications, ranging from catalysis and sensing to nanoelectronics and biomedical imaging but is not without its limitations and challenges. One of the primary difficulties lies in controlling the uniformity and precision of the assemblies, as electrostatic interactions are highly sensitive to minor changes in environmental conditions such as ionic strength, and temperature. This sensitivity can lead to irregular or non-uniform assemblies, reducing reproducibility and precision. Moreover, the stability of these assembled structures is often limited; they can disassemble or aggregate over time, especially when exposed to fluctuating environmental conditions, which poses a significant challenge for applications requiring long-term stability. Another limitation is the narrow range of conditions in which this self-assembly process is effective. Outside specific ionic strengths, the electrostatic forces may either be too weak to induce assembly or too strong, leading to unwanted aggregation. This restricts the versatility of the method across different environments or applications. Additionally, in complex solutions, competing interactions such as van der Waals forces, steric hindrance, or specific chemical interactions can interfere with the electrostatic self-assembly, making it difficult to achieve consistent and predictable outcomes. Scaling up the self-assembly of gold nanoparticles *via* electrostatic interactions presents another challenge, particularly due to charge screening in high ionic strength environments. As ionic strength increases, the Debye length shortens, reducing the effectiveness of electrostatic forces and leading to inconsistent or uncontrolled assembly. This variability, coupled with the sensitivity of the assemblies to external conditions like temperature and mechanical stress, compromises their structural integrity and limits practical applications. Additionally, the need for specific surface charges restricts functionalization flexibility, further constraining the ability to tailor assemblies for specific purposes. These challenges underscore the need for optimized strategies to improve the stability and scalability of gold nanoparticle assemblies. In summary, the chemistry of 2D monolayer films of Au-NPs assembled *via* electrostatic interactions represents a rich area of research with broad implications. Through a detailed understanding of the underlying mechanisms and careful control over experimental parameters, researchers can harness electrostatic forces to create functional nanomaterials with tailored properties and enhanced performance.

2.2. Van der Waals interactions

Experimentally the formation of 2D monolayer films of Au-NPs *via* van der Waals forces represents a fascinating area of study within nanomaterials chemistry. Van der Waals interactions, which encompass dispersion forces and induced dipole–dipole

interactions, play a crucial role in mediating the assembly of Au-NPs into ordered arrays on a substrate. This assembly mechanism relies on the weak, non-covalent interactions between neighboring nanoparticles, which allow them to adhere to each other and to the substrate surface, forming stable monolayer films. The detailed mechanism of assembly *via* van der Waals forces involves several key steps. Initially, Au-NPs dispersed in solution are brought into close proximity with a substrate, typically through methods such as drop-casting or spin-coating. As the solvent evaporates, the nanoparticles undergo Brownian motion and become confined to the substrate surface. Van der Waals interactions between adjacent nanoparticles promote their lateral aggregation, leading to the formation of compact monolayer films. The morphology and packing density of these films can be influenced by factors such as nanoparticle size, shape, and surface chemistry.

Several studies have explored the role of van der Waals forces in the assembly of 2D Au-NP monolayer films and compared them with other assembly mechanisms. For instance, Wang *et al.* (2019)[8] investigated the assembly of Au-NPs on various substrates and found that van der Waals interactions dominated the assembly process, particularly in systems with low surface energy. They demonstrated that by tuning the substrate properties and nanoparticle concentration, it was possible to control the morphology and structural integrity of the resulting monolayer films. Similarly, Li *et al.* (2020)[9] compared the assembly kinetics of Au-NPs driven by van der Waals forces *versus* electrostatic interactions and found that while both mechanisms contributed to nanoparticle aggregation, van der Waals forces played a predominant role in determining the final film structure. Further insights into the mechanism of assembly *via* van der Waals forces have been gained through advanced characterization techniques such as atomic force microscopy (AFM) and scanning tunneling microscopy (STM). These techniques enable researchers to directly visualize the arrangement of nanoparticles within the monolayer films and to quantify parameters such as particle size, spacing, and orientation. The assembly of 2D monolayer films of Au-NPs *via* van der Waals forces can be described by theoretical models based on interparticle interactions. One such model is the Derjaguin–Landau–Verwey–Overbeek (DLVO) theory, which considers both attractive van der Waals forces and repulsive electrostatic forces between nanoparticles. The total interaction energy (U) between two Au-NPs can be expressed as:

$$U = U_{\mathrm{vdW}} + U_{\mathrm{elec}} \quad (1)$$

Where U_{vdW} represents the van der Waals interaction energy and U_{elec} represents the electrostatic interaction energy. The van der Waals interaction energy U_{vdW} can be calculated using the Hamaker constant (A) and the separation distance (d) between nanoparticles:

$$U_{\mathrm{vdW}} = -6d^2A \quad (2)$$

Additionally, the electrostatic interaction energy U_{elec} can be described using the classical DLVO expression:

$$U_{\mathrm{elec}} = 4\pi\epsilon_0\epsilon_r dZ_1Z_2e^2 \quad (3)$$

Where Z_1 and Z_2 are the charges on the nanoparticles, (e) is the elementary charge, (ϵ_0) is the vacuum permittivity, (ϵ_r) is the relative permittivity of the medium, and (d) is the separation distance between nanoparticles.

In comparison with the literature, experimental observations of nanoparticle assembling kinetics and film morphology can be interpreted in the context of theoretical models such as DLVO theory. For example, studies by Wang *et al.* (2019)[8] and Li *et al.* (2020)[9] have demonstrated a good agreement between experimental data and theoretical predictions, supporting the importance of van der Waals forces in driving nanoparticle aggregation and film formation. By correlating experimental observations with theoretical models of van der Waals interactions, researchers can deepen their understanding of the assembling process and optimize conditions for the fabrication of tailored Au-NP monolayer films with desired properties. In summary, the chemistry of 2D monolayer films of Au-NPs assembled *via* van der Waals forces offers a versatile platform for engineering functional nanomaterials. By exploiting weak, non-covalent interactions between nanoparticles, researchers can achieve precise control over the structure and morphology of the resulting films, paving the way for applications in catalysis, sensing, and nanoelectronics.

2.3. Ligand-mediated interactions

The chemistry underlying the formation of 2D monolayer films of Au-NPs *via* ligand-mediated interactions involves the interplay of various forces, including covalent bonding and non-covalent interactions between ligands and substrate surfaces. Thiol-based ligands, commonly used to functionalize Au-NP surfaces, forming robust covalent bonds with gold atoms on the nanoparticle surface. This chemistry can be described by the following general reaction:

$$\mathrm{Au–S + Au–S \rightarrow Au–S–Au + S} \quad (4)$$

Here, Au–S represents the thiol ligand bound to the gold surface, and Au–S–Au represents the bridging ligand formed when two Au-NPs are brought into close proximity on the substrate surface. The assembly mechanism *via* ligand-mediated interactions can be further understood through theoretical models and experimental studies. For instance, the Langmuir–Blodgett technique involves the transfer of Au-NPs from a liquid subphase onto a solid substrate, facilitated by the formation of a monolayer at the air–water interface. The surface pressure (Π) exerted during compression of the monolayer can be described by the equation:

$$\Pi = F/A \quad (5)$$

Where (F) is the force applied perpendicular to the surface, and (A) is the area of the surface. By controlling the compression process, researchers can achieve precise control over the packing density and morphology of the resulting monolayer films. Another example, the "grafting to" approach involves the

direct attachment of pre-synthesized ligand-functionalized Au-NPs onto a substrate modified with complementary ligands. In contrast, the "grafting from" approach involves the *in situ* growth of ligands on the substrate surface followed by the addition of Au-NPs. These assembly strategies offer different levels of control over the nanoparticle packing density and morphology, depending on factors such as ligand density, chain length, and solvent conditions.

In the literature, numerous studies have investigated the role of ligand-mediated interactions in the assembly of 2D Au-NP monolayer films and compared them with other assembly mechanisms. For instance, Liu *et al.* (2017)[10] demonstrated the fabrication of highly ordered Au-NP monolayer films using a combination of self-assembly and surface-initiated polymerization techniques. They found that the density and orientation of the Au-NPs could be precisely controlled by adjusting the polymer brush thickness and surface coverage. Similarly, Zhang *et al.* (2019)[11] reported the formation of Au-NP monolayer films with tunable plasmonic properties through the selective replacement of ligands on the nanoparticle surface. Further insights into the mechanism of assembly *via* ligand-mediated interactions have been gained through advanced characterization techniques such as X-ray photoelectron spectroscopy (XPS) and Fourier-transform infrared spectroscopy (FTIR). These techniques allow researchers to probe the chemical composition and structure of the assembled monolayer films, providing valuable information about the interactions between the ligands and the substrate surface. By correlating experimental observations with theoretical models, researchers can develop strategies to optimize the assembly process and tailor the properties of Au-NP monolayer films for specific applications, ranging from catalysis and sensing to nanoelectronics and biomedicine. In summary, the chemistry of 2D monolayer films of Au-NPs assembled *via* ligand-mediated interactions offers a versatile platform for engineering functional nanomaterials. By harnessing the strong binding affinity between thiol-based ligands and gold surfaces, researchers can achieve precise control over the structure and properties of the resulting films, opening up new opportunities for the development of advanced nanotechnologies.

3. Size-dependent formation of 2D monolayer films of Au-NPs

Understanding the formation of 2D monolayer films of Au-NPs is crucial for tailoring their properties and optimizing their applications. This phenomenon is intricately linked to the size of the nanoparticles and involves a complex interplay of forces during self-assembly. The mechanism of size-dependent formation involves several key steps. Initially, Au-NPs are synthesized through methods like the Turkevich or citrate reduction method, yielding nanoparticles with different sizes. Upon dispersion onto a substrate, such as a silicon wafer or mica, the nanoparticles self-assemble due to various forces, including van der Waals (F_{vdW}), electrostatic (F_{elec}), and steric (F_{steric}) interactions. Detailed studies have elucidated the role of nanoparticle size in the formation of 2D monolayer films. For instance, the Langmuir adsorption isotherm equation,

$$\Gamma = C_{eq}A/RT \quad (6)$$

where Γ is the surface coverage, (C_{eq}) is the equilibrium concentration of Au-NPs, (A) is the area per nanoparticle, (R) is the gas constant, and (T) is the temperature. The equation has been used to describe the adsorption process. Zhang *et al.* (2012)[12] demonstrated that smaller Au-NPs tend to form denser monolayers compared to larger nanoparticles. This size-dependent behavior is attributed to the increased surface area of smaller nanoparticles, leading to stronger interparticle interactions and closer packing. Additionally, larger nanoparticles may exhibit a greater tendency to aggregate due to decreased surface-to-volume ratio.

The monolayer formation process involves the adsorption of Au-NPs onto the substrate surface, followed by their diffusion and rearrangement to minimize the system's free energy. Theoretical models, such as Monte Carlo simulations, have been employed to understand the kinetics and thermodynamics of this process. For instance, a study by Nie *et al.* (2017)[13] utilized Monte Carlo simulations to investigate the effect of nanoparticle size and substrate interaction on the self-assembly process. They found that smaller nanoparticles exhibit faster diffusion and higher mobility on the substrate, leading to more rapid monolayer formation. Comparisons with literature highlight the complex interplay among nanoparticle size, surface chemistry, and substrate properties in monolayer formation. For example, a study by Liu *et al.* (2019)[14] explored the influence of surface ligands on the self-assembly behavior of Au-NPs. They found that modifying the surface chemistry of nanoparticles can alter their interaction strength and packing density on the substrate, thereby affecting the morphology of the resulting monolayer. Overall, understanding the size-dependent formation of 2D monolayer films of Au-NPs is essential for tailoring their properties and optimizing their performance in various applications. The major challenges in forming Au-NPs monolayers due to size influence include achieving uniform coverage, as smaller NPs tend to aggregate and larger ones may settle in clusters. Electrostatic repulsion is more pronounced for smaller particles, complicating uniform deposition, while larger particles face alignment and packing issues. Diffusion rates differ with size, affecting assembly dynamics and potentially leading to non-uniform layers. Mechanical instability in smaller NPs can cause defects, while larger particles may require precise field strength for effective deposition. Variability in surface chemistry and the need for optimized synthesis parameters further complicate the process, and accurate characterization of monolayers is challenging due to size-dependent behaviors.

4. Shape-dependent formation of 2D monolayer films of Au-NPs

The formation of 2D monolayer films of Au-NPs is also intricately influenced by their shape, which plays a pivotal role in tailoring their functionalities across various fields such as catalysis, sensing, and biomedicine. The mechanism governing

shape-dependent formation involves a complex interplay of forces during self-assembly onto a substrate. Synthesis methods, such as seed-mediated growth or template-assisted synthesis, yield Au-NPs with distinct shapes, such as spheres, rods, or triangles, each exhibiting unique self-assembly behavior. Research exploring the shape-dependent formation of Au-NP monolayers has provided valuable insights into assembly kinetics and thermodynamics. For instance, Studies by Smith *et al.* (2015)[15] revealed that the shape of Au-NPs significantly impacts their packing density and arrangement in monolayer films. Anisotropic nanoparticles, such as rods or triangles, often form more ordered assemblies compared to spherical counterparts due to their distinct surface properties and aspect ratios. Wang *et al.* (2020)[16] explored the influence of solvent properties on the self-assembly behavior of Au-NPs with various shapes. Their findings emphasized the importance of solvent characteristics in modulating nanoparticle interactions and monolayer structure. Understanding the shape-dependent formation of 2D monolayer films of Au-NPs holds immense significance for tailoring their properties and functionalities across diverse applications. By elucidating the underlying mechanisms and drawing comparisons with existing literature, researchers can advance the design and optimization of Au-NP-based materials with enhanced performance and versatility.

Shape-dependent challenges in forming Au-NPs monolayers include difficulties in achieving uniform alignment and packing, as non-spherical particles often result in irregular deposition. Variations in surface interactions due to anisotropic shapes can lead to uneven monolayer formation. Assembly dynamics are complicated by shape-induced anisotropy, which may cause incomplete or non-uniform coverage. Additionally, non-spherical particles may exhibit varying mechanical stability, affecting the monolayer's integrity. The influence of electrostatic and van der Waals forces can differ with particle shape, complicating deposition, while the orientation of the electric field relative to the particles also needs careful control to ensure consistent results.

5. Different interfaces of Au NPs monolayer

Au-NPs monolayers can form various interfaces depending on their arrangement and the surrounding environment. The formation of Au-NP monolayers at the air–liquid–solid interface is a complex and fascinating process driven by interfacial forces and molecular interactions. This process involves the interplay between three phases: air, liquid, and solid, and the self-assembly is influenced by the chemistry of the ligands or surfactants on the Au-NP surfaces. These ligands typically possess hydrophobic alkyl chains and hydrophilic functional groups, providing the nanoparticles with amphiphilic characteristics. When a dispersion of Au-NPs is applied to a water surface in contact with a solid substrate, the hydrophobic tails of the ligands orient towards the air to avoid contact with water molecules, while the hydrophilic heads remain in the aqueous phase, facilitating the assembly at the interface.

5.1. Gas–water interface

The formation of Au-NP monolayers at the gas–water interface is an intriguing phenomenon driven by interfacial forces and molecular interactions. The chemistry of this self-assembly process centers around the ligands or surfactants attached to the Au-NP surfaces. These ligands typically have hydrophobic alkyl chains and hydrophilic functional groups, giving the nanoparticles amphiphilic properties. When a dispersion of Au-NPs is introduced to the water surface, the hydrophobic tails of the ligands orient toward the air phase to avoid contact with water molecules, while the hydrophilic heads remain in the aqueous phase. This alignment facilitates the spontaneous formation of a densely packed monolayer of Au-NPs at the interface. Understanding the underlying thermodynamic and kinetic processes is essential for optimizing the conditions needed to achieve stable and high-quality monolayers.

5.1.1. Thermodynamic considerations. From a thermodynamic standpoint, the Gibbs free energy (ΔG) of Au-NPs at the air–water interface can be calculated using the equation:

$$\Delta G = -\pi R^2 \gamma_{\text{air/water}} (\cos\theta - 1)^2 \quad (7)$$

where: θ is the contact angle of Au-NPs in aqueous solution, R is the particle radius, $\gamma_{\text{air/water}}$ is the interfacial tension between air and water.

This equation shows that ΔG is always negative, indicating that the transfer of Au-NPs to the air–water interface reduces Gibbs free energy. Consequently, this process is thermodynamically spontaneous regardless of the hydrophobicity of the Au-NPs. Therefore, the transfer of Au-NPs from the solution to the interface is inherently favorable.

5.1.2. Kinetic considerations. Despite favorable thermodynamics, the spontaneous assembly of Au-NPs at the interface is often hindered by kinetic barriers. The primary kinetic obstacle is the high sorption potential barrier (G), which impedes the adsorption of particles onto the interface. Overcoming this barrier typically requires additional driving forces. Experimental studies and simulations have identified several effective strategies for reducing the sorption barrier and promoting assembly: (1) addition of electrolytes: – electrolytes lower the surface charge density of Au-NPs, reducing electrostatic repulsion and facilitating assembly. Initially, strong electrolytes were used, but they often led to bulk coagulation, making the process uncontrollable. A more refined approach involves using weak electrolytes. (2) Hydrophobic modification: – enhancing the hydrophobicity of Au-NP surfaces increases their affinity for the air–water interface, promoting self-assembly. (3) Surface active solvents: – using solvents that reduce interfacial tension can also help overcome kinetic barriers, leading to more efficient assembly. These methods underscore the need to balance thermodynamic driving forces with kinetic facilitators to achieve optimal monolayer formation.

5.1.3. Applications and further research on air–water interface Au-NPs monolayer assembly method. The properties and stability of Au-NP monolayers at the air–water interface are influenced by various factors, including the length and

structure of the ligands, the size and shape of the nanoparticles, and the surface tension of the water. For instance, longer alkyl chains and stronger hydrophobic interactions typically result in more stable monolayers with higher packing densities. Numerous studies have explored the self-assembly behavior and properties of Au-NP monolayers at the air–water interface. For example, Huang *et al.* (2015)[17] investigated how ligand chemistry and nanoparticle size affect the stability and packing density of Au-NP monolayers. They discovered that longer alkyl chain ligands produced more stable monolayers with higher packing densities, enhancing surface properties. Additionally, Smith *et al.* (2018)[18] used *in situ* techniques to study the dynamics of Au-NP monolayers at the gas–water interface. They observed the formation of dynamic domains within the monolayer and elucidated the mechanisms underlying nanoparticle rearrangement at the interface. Understanding the chemistry and properties of Au-NP monolayers at the air–water interface is crucial for various applications, including surface engineering, biosensing, and colloidal stabilization. Continued research in this area could lead to the development of advanced materials and technologies with tailored interfacial properties for specific applications. By integrating thermodynamic and kinetic insights with practical strategies for reducing kinetic barriers, researchers can better control the formation of 2D Au monolayers at the air-liquid interface. This comprehensive understanding is essential for advancing applications in catalysis, sensing, and nanoelectronics.

5.2. Solid substrate interface

At the interface with a solid substrate, monolayers of Au-NPs are formed through intricate self-assembly processes governed by interparticle interactions and interfacial forces with the substrate surface. The underlying chemistry involved in this assembly hinges upon a complex interplay of factors, including the surface chemistry of the substrate, the composition of ligands or surfactants coating the Au-NPs, and the solvent environment in which the assembly takes place. Typically, Au-NPs are dispersed within a solvent and carefully deposited onto the surface of the solid substrate. Here, they undergo a process of self-organization, driven by a delicate balance of attractive and repulsive forces. The ligands or surfactants surrounding the Au-NPs play a pivotal role in mediating these interactions, offering stability and exerting control over the assembly dynamics.

A breadth of research has delved into unraveling the intricacies of self-assembly behaviors and properties exhibited by Au-NPs monolayers at the solid substrate interface. Notably, investigations by Lee *et al.* (2016)[19] have probed into the influence of substrate chemistry and nanoparticle dimensions on the morphology and structural characteristics of resulting monolayers. Their findings illuminate how factors such as substrate hydrophobicity can drive closer packing of nanoparticles, thereby enhancing surface coverage and monolayer stability. Furthermore, the work of Zhang *et al.* (2019)[20] has shed light on the profound impact of solvent evaporation kinetics on assembly dynamics and monolayer structure. Their observations elucidate how varying rates of solvent evaporation yield differing levels of order and packing density within the monolayer, with slower evaporation fostering more organized and densely packed assemblies. Understanding the nuanced chemistry and inherent properties governing Au-NPs monolayers at the solid substrate interface holds paramount importance across a spectrum of applications, from precision surface patterning to the development of advanced nano electronic devices and catalytic systems.

5.3. Liquid–liquid interface

The phenomenon of self-assembly of Au-NPs into films at fluid interfaces has garnered considerable attention due to the inherent fluidity of the interface, which aids in the annealing of defects within the assembled film.[21] Various methodologies have been devised to transfer nanoparticles from colloidal solutions to fluid interfaces, involving the addition of inorganic or organic compounds to the aqueous colloid to either reduce the surface charge or thin the electrical double layer of nanoparticles.[22–25] One commonly employed technique utilizes ethanol as an economical reagent to extract nanoparticles from aqueous colloids to oil/water interfaces, resulting in the formation of large-area, close-packed nanoparticle monolayers.[25–27] However, the ethanol-mediated method has its drawbacks, notably the inclusion of toluene or heptane and the disruptive nature of gradual ethanol addition. The use of toluene or heptane, particularly toluene, poses health risks to operators and is unsuitable for large-scale production of nanoparticle films. Additionally, the gradual addition of ethanol constantly disturbs the assembling location for nanoparticles, *i.e.*, the interface, leading to the formation of large voids and three-dimensional (3D) aggregates within the resulting monolayer. To address these limitations, Min-Hua Wang *et al.*[28] devised a method to fabricate close-packed Au-NP monolayers with sub-10 nm interparticle spacing by simply covering *n*-butanol on the surface of an Au aqueous colloid. This novel approach not only eliminates the need for hazardous substances like toluene or heptane but also circumvents the disruptive effects of gradual ethanol addition. Consequently, the resulting close-packed nanostructure can further transform into two-dimensional (2D) aggregates with varying degrees of aggregation upon aging for several days as shown in Fig. 3.

5.4. Gas–solid interface

The gas–solid interface assembly of Au-NPs monolayer is a sophisticated technique used to create a uniform, single layer of nanoparticles on a solid substrate, significant for various applications such as catalysis, sensing, and electronic devices. Au-NPs are typically synthesized using chemical reduction methods like the Turkevich method, where gold salts are reduced by agents such as citrate, forming colloidal Au-NPs. To ensure stability and facilitate controlled interaction with the substrate, these nanoparticles are often functionalized with ligands, including thiols, amines, or polymers, which prevent aggregation and enhance substrate affinity. Substrate preparation is crucial and involves meticulous cleaning and sometimes

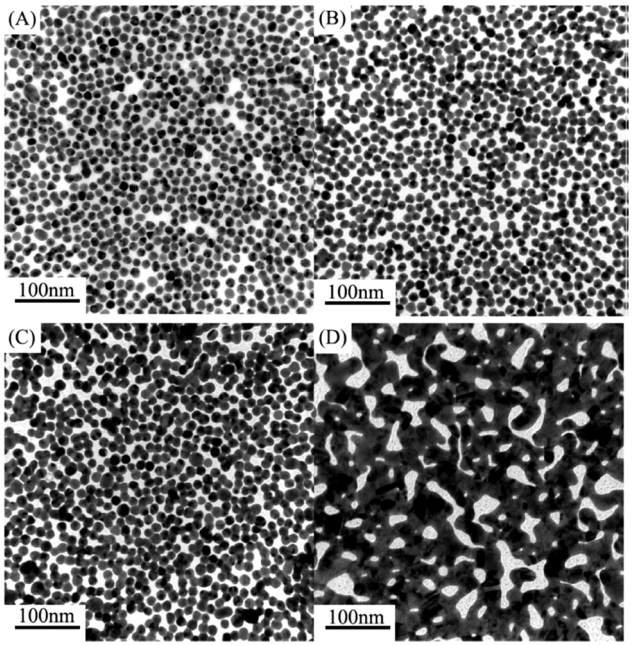

Fig. 3 TEM images of Au-NP monolayers: (A) without aging, (B) aging for 3 days, (C) aging for 7 days, and (D) aging for 10 days. Reproduced from ref. 28 with permission from [IOP Publishing], copyright [2010].

modification to increase surface energy and promote nanoparticle adhesion. Common techniques for assembling a monolayer of Au-NPs at the gas–solid interface include the Langmuir–Blodgett (LB) method, drop-casting, spin coating, and self-assembly from the vapor phase. The LB method forms a monolayer at the air–water interface, which is then transferred to the substrate. Drop-casting involves placing a colloidal solution on the substrate and allowing the solvent to evaporate, although this can result in non-uniform layers due to the "coffee-ring effect," where particles accumulate at the edges of the droplet. Spin coating uses centrifugal force to spread the solution uniformly, while self-assembly from the vapor phase deposits nanoparticles as the solvent vapor condenses on the substrate. During deposition, Au-NPs adsorb onto the substrate due to van der Waals forces, electrostatic interactions, or specific binding interactions between the ligands and the substrate. Post-assembly treatments such as annealing and chemical modification can further enhance the monolayer's properties. Annealing improves adhesion and removes residual solvents, while chemical modification tailors surface properties for specific applications. Wang's team[29] reported significant variations in the final assembled morphologies of Au-NPs depending on their shapes. They also highlighted that adjusting the droplet size is an effective strategy to mitigate the coffee-ring effect. When the droplet size is relatively small, it evaporates quickly, leaving insufficient time for the solute to migrate to the edges. Conversely, Wong and colleagues[30] observed that the coffee-ring effect becomes more pronounced as the droplet size increases. Furthermore, strengthening the interactions between Au-NPs can help to diminish the capillary flow, further reducing the coffee-ring effect.

5.5. Electric field driven assembly of Au-NPs monolayer

In addition to shape and droplet size, other factors influencing the assembly of Au-NPs include solvent properties, substrate characteristics, presence of surfactants and the electric field. Firdous Ahmad Deader[31] has reported a novel physical fabrication method for forming monolayers of Au-NPs on planar silicon surfaces using an electric field. By creating an electric field of 5.71×10^4 V m^{-1} between the parallel plates of a capacitor and applying a DC voltage, this technique effectively guides the self-assembly of nanoparticles. The Au-NPs, with a diameter of 20 nm and a zeta potential ranging from −250 to −290 mV, are influenced by the externally applied electric field, which drives their orderly deposition on the silicon substrate. The mechanism behind this monolayer formation was further analyzed using finite element simulation, revealing that the enhanced electric field around the Au-NPs reaches an order of 10^8 V m^{-1}. This intense field indicates a high surface charge density on the nanoparticles, resulting in a significant electric force per unit area that aids in their uniform settlement on the silicon surface. The detailed process of Au-NP deposition on the silicon substrate includes setting up the experiment by placing a drop of Au-NP solution in the electric field created between the parallel plates of a capacitor, as depicted in Fig. 4. Side and top views show the monolayer formation under the influence of the electric field and the diffusion of Au-NPs. This electric field-driven self-assembly technique is significant for several reasons: it ensures a highly uniform monolayer of Au-NPs, which is crucial for applications requiring consistent surface properties; it is scalable and reproducible with high precision, making it suitable for industrial applications; and it is versatile, potentially adaptable for other substrates, broadening its applicability. The development of this technique opens up new possibilities in nanotechnology and material science. Future research could focus on optimizing electric field parameters and nanoparticle properties to achieve even more precise control over the assembly process, exploring the combination of Au-NPs with other nanomaterials to create multifunctional surfaces with enhanced properties, and applying this technique in fields such as electronics, photonics, and biosensing, where uniform and well-ordered nanoparticle layers can lead to significant advancements. In summary, the electric field-driven self-assembly method developed by Firdous Ahmad Deader *et al.* represents a promising approach for fabricating highly uniform monolayers of gold nanoparticles on silicon substrates. This technique's scalability, precision, and potential for adaptation make it a valuable tool in the advancement of nanotechnology and its applications.

5.6. Chemical exfoliation method

In 2024 Shun Kashiwaya *et al.*[32] reported a novel synthetic pathway, which has been devised to exfoliate goldene from Ti_3AuC_2, a nano-layered MAX phase consisting of transition metal (M), group A element (A), and either carbon (C) or nitrogen (N) (initially formed by substituting Au for Si in Ti_3SiC_2), as shown in Fig. 5. This process involves wet-chemical etching of the carbide layers using Murakami's reagent, employing cetrimonium bromide (CTAB) or cysteine. Notably,

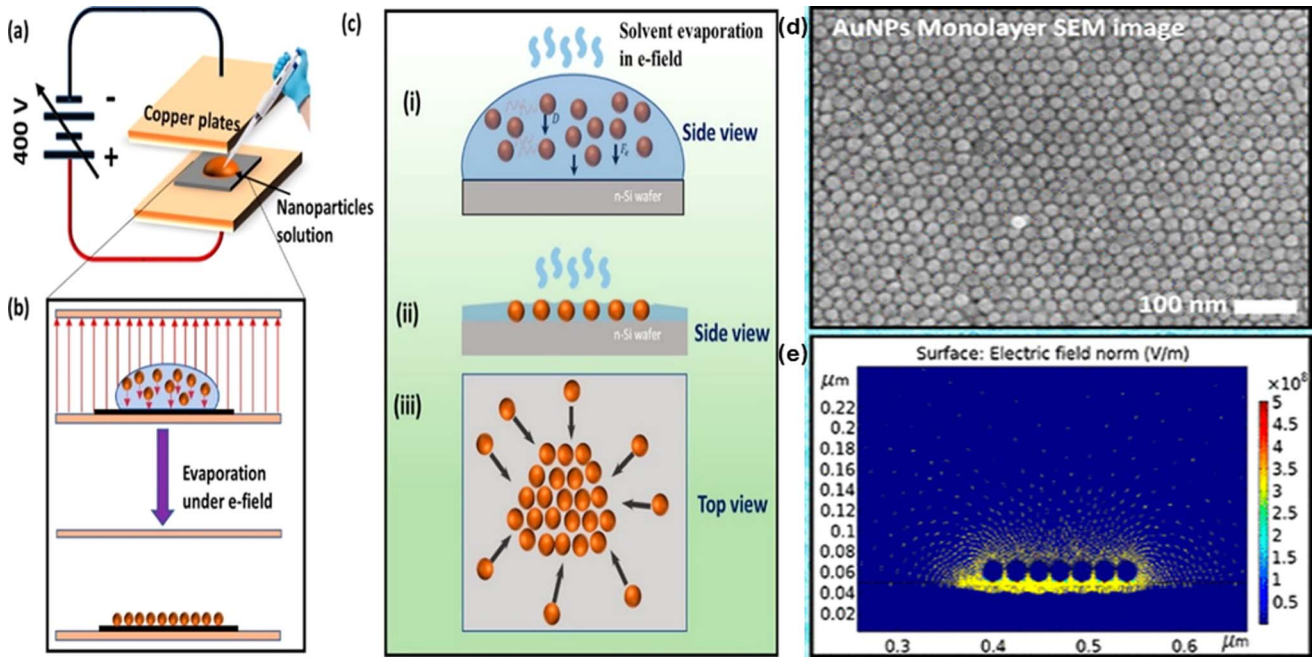

Fig. 4 Outlines the Au-NP deposition process on a silicon substrate. (a) Shows the experimental setup for NP deposition under an electric field. (b) Provides a schematic of the monolayer formation of Au-NPs on the substrate. (c) Depicts both side and top views of the monolayer formation influenced by the electric field and NP diffusion, (d) SEM image and (e) COMSOL simulation of electric field effect on the negatively charged Au-NPs. Reproduced from ref. 31 with permission from [ACS Publications], copyright [2023].

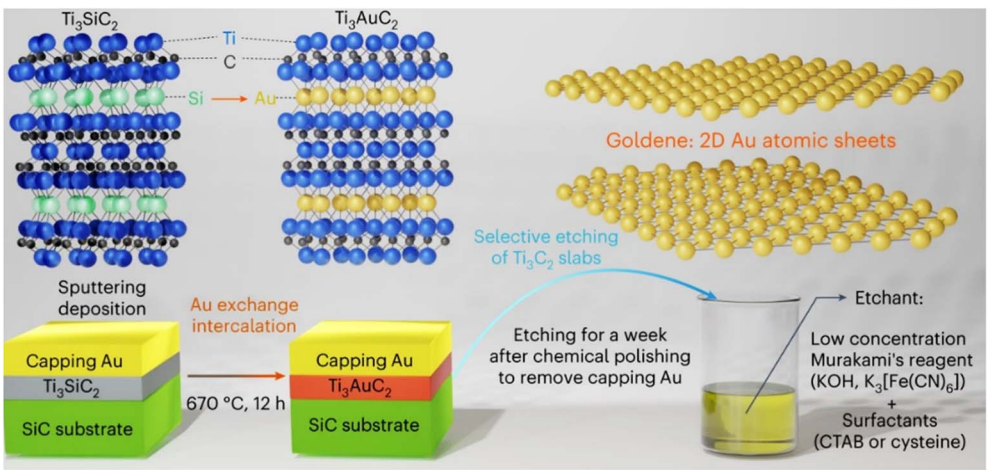

Fig. 5 Preparation of goldene material *via* chemical exfoliation method. Reproduced from ref. 32 with permission from [Springer Nature], copyright [2024].

this method is both straightforward and scalable, and importantly, it does not involve the use of hydrofluoric acid.

The etching mechanism facilitated by Murakami's reagent stems from the generation of radical nascent oxygen [O] during the reaction between potassium ferricyanide and alkali in close proximity to the surface of metal carbides, which exhibits an affinity for oxygen. When the surface is exposed to potassium ferricyanide ($K_3[Fe(CN)_6]$) and KOH, the Ti_3C_2 slabs absorb nascent oxygen from KOH, leading to the formation of potassium ferrocyanide ($K_4[Fe(CN)_6]$) as a by-product. Subsequently, Ti_3C_2 slabs undergo oxidation by nascent oxygen, with Ti and C being selectively oxidized due to their higher ionization tendency and susceptibility to oxidation compared to Au.

$$4K_3[Fe(CN)_6] + 4KOH \rightarrow 4K_4[Fe(CN)_6] + 2H_2O + 2[O] \quad (8)$$

$$2Ti_3C_2 + 11[O] \rightarrow 3Ti_2O + 4CO_2$$

$$2Ti_3C_2 + 7[O] \rightarrow 3Ti_2O + 4CO$$

$$2Ti_3C_2 + 3[O] \rightarrow 3Ti_2O + 4C$$

In contrast, Au remains inert to both potassium ferricyanide and potassium ferrocyanide in darkness, but light-triggered dissolution of Au by potassium ferrocyanide has been observed. Given this, the preparation of Murakami's reagent was conducted under minimal ambient light, and etching was performed in complete darkness to prevent the evolution of cyanide, which can attack Au. Consequently, the susceptibility of Ti_3C_2 slabs to oxidation outweighs that of Au, which remains negligible under the dark conditions employed in this study.

To prevent the coalescence of goldene layers and stabilize them, Murakami's reagent was supplemented with various surfactants such as CTAB, cysteine, and cysteamine. CTAB, a common surfactant, forms a bilayer on the Au surface, hindering the agglomeration of Au nanoparticles. Cysteine and cysteamine, characterized by thiol and amine functional groups, respectively, are utilized to stabilize and functionalize planar gold surfaces. The thiol group of cysteine, when attached to the Au surface, exhibits greater resistance to oxidation compared to cysteine located further away from Au. Excess cysteine and cysteamine, not reaching the Au surface, are prone to oxidation by nascent oxygen, forming disulfide by-products. These larger disulfide molecules are less likely to diffuse between goldene layers during etching of the intercalated MAX-phase host, while their affinity towards Au surfaces persists due to the presence of amine functional groups. Consequently, goldene layers are predominantly observed near the edges of MAX phases where larger surfactants can penetrate between Au layers. Observations through electron microscopy reveal goldene layers exhibiting approximately 9% lattice contraction compared to bulk gold. While atomistic simulations demonstrate goldene's inherent stability in two dimensions, experimental results indicate some degree of curling and agglomeration. However, the addition of surfactants proves effective in stabilizing the exfoliated goldene derived from Au-intercalated MAX phases, thus mitigating these tendencies. Further analysis utilizing X-ray photoelectron spectroscopy (XPS) elucidates a notable shift in the Au 4f peak towards higher binding energy (E_b) by 0.88 eV, providing valuable insights into the electronic structure of the exfoliated goldene material.

5.7. Electrophoretic deposition (EPD)

The Electrophoretic deposition (EPD) method is known as directed assembly, stands out for its array of advantages. Notably, it possesses rapid processing capabilities and exhibits remarkable versatility, accommodating various particle types and substrates with ease.[33–37] Additionally, its utilization necessitates uncomplicated apparatus and entails straightforward application procedures. A standard EPD process for fabricating 15 nm thin films can be completed within a few minutes, showcasing its efficiency. Moreover, the precision of film thickness is achievable through meticulous adjustment of EPD parameters such as applied voltage, particle concentration, and deposition duration. EPD has garnered recognition as a versatile technique applicable to an extensive array of materials, spanning ceramic powders, metallic particles, polymers, and semiconductor materials. Noteworthy studies by Shah *et al.*[38,39] have delved into the assembly of colloidal microcrystals and liquid crystals under direct current electric fields, while seminal work by Prieve *et al.*[40,41] has contributed fundamental theories underpinning nanoparticle EPD assembly. These investigations underscore EPD's potential as a promising avenue for generating nanomaterial patterns. However, despite its promise, EPD's application in nanoscale assembly remains a formidable challenge. While previous efforts have predominantly focused on depositing larger micrometer-scale particles, endeavors to extend EPD to nanoscale assembly encounter significant hurdles. Brownian motion poses a substantial impediment to precise particle deposition, while the influence of double layer effects on nanoparticle-surface interactions further complicates the process. Additionally, the inability to observe single nanoparticles during deposition exacerbates the challenge of optimizing the assembly process.

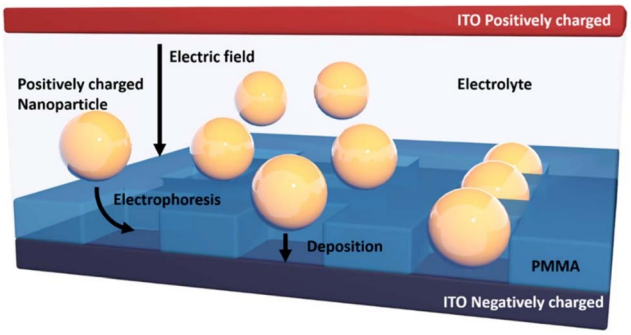

Fig. 6 Schematic of the EPD process showing nanospheres deposited onto EBL fabricated ITO–PMMA template. Reproduced from ref. 44 with permission from [ACS Publications], copyright [2018].

Although seminal studies, such as those by Barbee *et al.*[42] and Qian *et al.*,[43] have demonstrated the feasibility of EPD in depositing micrometer-scale particles into defined patterns, achieving single nanoparticle resolution and orientational control remains elusive as shown in Fig. 6. While reports provide proof-of-concept for combining EPD with patterned templates for particle assembly, scaling down to the nanoscale presents formidable obstacles. Nonetheless, addressing these challenges holds the potential for groundbreaking advancements in nanomaterial assembly techniques.[45] Heyou Zhang *et al.*[44] have demonstrated a highly efficient method for large area assembly of single gold nanoparticles (spheres – 30 nm in size and rods – <100 nm in length) into a prepatterned poly(-methyl methacrylate) (PMMA)–indium tin oxide (ITO) template *via* EPD. As a consequence of the pre-treatment applied to the patterned substrate, the Au-NPs exhibited remarkable attributes of selectivity and uniformity upon deposition.

5.8. *In Situ* reduction

One of the critical methods for enhancing the functionality of Au-NPs is through the creation of well-ordered monolayers and

controlled assemblies. In particular, the *in situ* reduction assembly technique has emerged as a pivotal method for fabricating these structures directly on various substrates, offering numerous advantages such as uniformity, high surface coverage, and enhanced stability. *In situ* reduction involves the chemical reduction of gold precursors directly on the substrate surface, leading to the formation of Au-NPs that are tightly bound and well-distributed. This approach not only simplifies the fabrication process but also ensures that the nanoparticles are formed in a controlled manner, allowing for precise tuning of their size, shape, and distribution. The resulting gold monolayers exhibit excellent properties for applications in sensing, where the uniformity and density of the nanoparticles are crucial for achieving high sensitivity and specificity. Yi-Wen Wang[46] recently reported a novel method for growing wafer-sized continuous mesoporous silica thin films (MSTFs) with well-ordered perpendicular nanochannels on various substrates, ranging from hydrophobic to hydrophilic surfaces, which could be used as a template for gold nanoparticle arrays. As shown in Fig. 7, By utilizing these MSTFs, a new technique was developed to create 2D Au-NPs arrays atop mesoporous channels with 2 nm nanogaps through a straightforward chemical reduction process.

In addition to MSTFs, mesoporous silica nanoparticles (MSNs) have also been employed as templates to fabricate densely coated periodic Au arrays on their external surfaces. These on-substrate mesoporous silica-templated gold nanoparticle arrays can be directly utilized for surface-enhanced Raman spectroscopy (SERS) applications without the need for transferring procedures, highlighting their practicality and efficiency. Fig. 8 shows SEM images of APTMS-functionalized structures: (a) MSTF and (d) spin-coated MSN on silicon wafers; high and low-magnification images (b and c) of MSTF-Au; and (e and f) MSN-Au, showing dense Au-NPs. Here, the gold nanoparticle arrays on MSTF and MSN were labeled as MSTF-Au and MSN-Au, respectively. Prior to gold reduction, both APTMS-functionalized mesoporous materials exhibited well-ordered mesostructures and fully accessible perpendicular nanochannels (Fig. 8a and d). After gold reduction, MSTF-Au (Fig. 8b) clearly shows periodic mesopores occupied by gold nanoparticles. This method leverages periodic mesopores as templates, resulting in centimeter-scale 2D gold nanoparticle arrays with an ultrahigh density of hot spots.

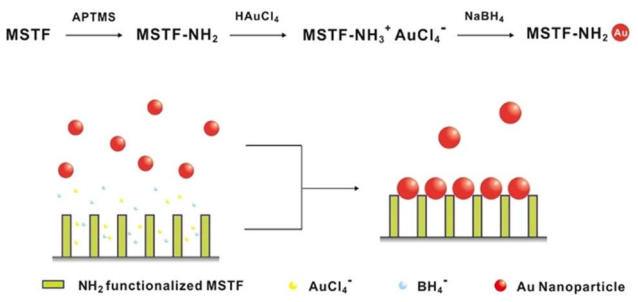

Fig. 7 Experimental approach for employing mesoporous silica thin film (MSTF) as a template to create gold nanoparticle arrays. Reproduced from ref. 46 with permission from [ACS Publications], copyright [2016].

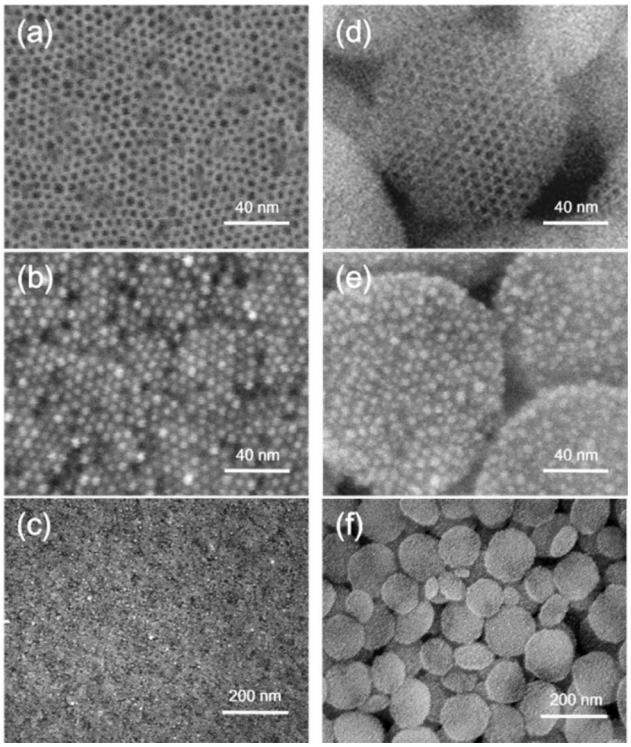

Fig. 8 SEM images of APTMS-functionalized structures: (a) MSTF and (d) spin-coated MSN on silicon wafers. High and low-magnification SEM images of (b and c) MSTF-Au and (e and f) MSN-Au, showing dense gold nanoparticles in the mesopores. Reproduced from ref. 46 with permission from [ACS Publications], copyright [2016].

The creation of Au-NP monolayers and arrays through *in situ* reduction and templating techniques opens new avenues for advanced sensing applications. In biosensors, these well-ordered structures can significantly enhance detection capabilities by providing numerous active sites and improving signal transduction. Furthermore, the ability to fabricate such arrays on a wide range of substrates expands their applicability in various fields, including environmental monitoring, medical diagnostics, and food safety. Future research may focus on further refining these techniques to achieve even greater control over nanoparticle properties and exploring new template materials to expand the range of possible applications. Additionally, integrating these gold nanoparticle assemblies with other nanomaterials and exploring their synergetic effects could lead to the development of next-generation multifunctional devices. In summary, the advancements in Au-NP monolayer fabrication and *in situ* reduction assembly techniques represent a significant step forward in nanotechnology, providing powerful tools for creating highly functional materials with broad application potential.

6. Applications of 2D monolayer of Au-NPs

6.1. Memory systems

The realm of flexible electronics has garnered significant attention due to their inherent advantages, such as being

lightweight, portable, and capable of bending. These properties make them highly suitable for a diverse range of applications, including large area displays, mobile phones, digital cameras, potable media players, laptop computers, sensor arrays, and radio frequency identification (RFID) tags. The effective implementation of flexible electronic solutions in these fields depends heavily on the development of non-volatile memory systems that offer reliable data storage and low production costs. In the field of non-volatile memories, several types have been investigated, each presenting unique features and challenges. These include ferroelectric memories, electret memories, resistive memories, and floating gate memories. Particularly noteworthy are nano-floating gate flash memory devices, which employ nanocrystals as charge trapping elements. These devices are preferred due to their straightforward architecture, non-destructive readout capabilities, and precise control over trap capacity.

Au-NPs are of particular interest for charge trapping in non-volatile memory devices, owing to their exceptional chemical stability and high work function. Numerous studies have highlighted the potential of Au-NPs to enhance memory performance. Despite these advancements, significant challenges remain, such as the need for high voltage operation and inadequate charge retention over extended periods. Overcoming these challenges is crucial for the advancement of flexible electronics. One promising strategy involves the careful selection of charge trapping sites and the optimization of dielectric materials.[47,48] By enhancing these components, it is possible to improve the performance and reliability of non-volatile memory devices. Continued research and development in this area are vital to surmount current limitations and fully exploit the potential of flexible electronic technologies. The impact of advancements in flexible electronics extends beyond consumer electronics, influencing fields such as healthcare, environmental monitoring, and wearable technology. For example, flexible sensors embedded in clothing can offer real-time health monitoring, and bendable displays can lead to innovative device designs. Thus, ongoing research and development in flexible electronics and related memory technologies are poised to drive significant technological progress across various industries.

To further advance these technologies, it is essential to create a high-quality nanoparticle monolayer and a dense tunneling dielectric that can effectively isolate trapped charges in discrete storage media, minimizing charge leakage. Additionally, a high dielectric constant (k) blocking layer is necessary to reduce operating voltage and power consumption. Consequently, developing a method to synthesize a well-dispersed nanoparticle monolayer within a high-k dielectric layer is crucial to prevent charge leakage. Moreover, it is imperative to conduct all fabrication processes at low temperatures to meet the requirements for constructing memory devices on flexible substrates. Given the importance of mechanical flexibility in flexible electronics, the charging behavior of memory devices under various bending conditions must be thoroughly investigated and understood for future applications. Furthermore, thermal modeling of organic devices is increasingly important as these devices are integrated into more complex systems where thermal-induced phenomena will play a significant role. Despite the importance of thermal properties in organic electronics, the thermal effects on the performance of organic memory devices with Au nanoparticle floating gates have not been systematically examined. Understanding the relationship between memory window, retention time, and operating temperature would be beneficial for comprehending the charge trapping mechanism. This knowledge is crucial for optimizing the performance and reliability of these innovative memory devices.

Ayman Rezk and colleagues[47] have demonstrated a metal-oxide-semiconductor (MOS) based nonvolatile memory element that utilizes isolated Au-NPs as storage sites. This innovative structure sandwiches the Au-NPs between amorphous aluminum oxide (Al_2O_3) thin films, which are deposited *via* atomic layer deposition to form the blocking and tunneling layers. The current–voltage characteristics during write/erase cycles were analyzed using conductive mode atomic force microscopy (C-AFM), which probes one isolated nanoparticle at a time. The consecutive voltage sweeps revealed a memory window in the I–V characterization, with an average voltage difference (ΔV) of 0.9 V at a reading current of 1.5 nA, indicating stored charge within the Au-NP. This charge originates from the AFM metal-coated probe. The results effectively demonstrate the writing and erasing operations of the device by charging and discharging a single Au-NP. Additionally, the underlying physics is discussed in terms of electric field enhancement due to charge confinement and its impact on conduction mechanisms. The schematics of the process flow for the fabricated nano memory devices and the circuit for probing a single Au-NP using C-AFM are illustrated in Fig. 9.

A notable effect of electron injection and trapping in a single Au-NP sandwiched between two ALD Al_2O_3 layers is observed when a positive voltage sweep from 0 to +3 V is applied to the substrate. A memory window of $\Delta V = 0.9$ V is observed for two consecutive voltage sweeps from −2 V to +3 V at a reading current of 1.5 nA. Moreover, the device with the structure Au-Tip/Al_2O_3/Au-NP/Al_2O_3/n-Si can be programmed and erased by applying a positive sweep (0 to +3 V) and a negative sweep (0 to −4 V), respectively. In contrast, the conventional MOS structure

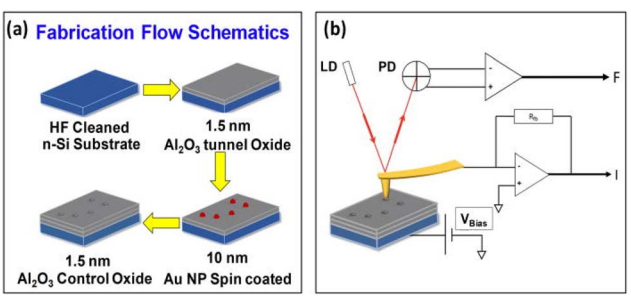

Fig. 9 (a) Fabrication process for nanomemory devices and (b) the circuit setup for probing a single Au-NP using conductive atomic force microscopy (C-AFM). Reproduced from ref. 47 with permission from [AIP Publishing], copyright [2020].

without Au-NPs shows no charging effect; instead, an abrupt current increase at an average set voltage of 3.2 V indicates filament formation due to the movement of oxygen vacancies. Finally, this single nanoparticle-based memory structure demonstrates lower power consumption compared to traditional resistance-based memory devices. Fig. 10 illustrates the energy band diagrams of the write/erase operations of the NP-based memory, showing the energy levels for different materials under zero bias, charge injection in the Au-NP under forward bias, and discharging of the Au-NP under negative bias. This innovative approach paves the way for the development of efficient, low power nano memory devices.

Ye Zhou *et al.*[49] have conducted an in-depth investigation into the strain and temperature-dependent memory effects of organic memory transistors fabricated on plastic substrates, under ambient conditions. In their study, an Au-NP monolayer was prepared and embedded within an Al_2O_3 layer deposited using atomic layer deposition, serving as the charge trapping layer. Fig. 11 gives a comprehensive view and characteristics of the flexible memory array: (a) three-dimensional illustration, (b) output characteristics and (c) energy diagram. These devices demonstrated low operational voltage, reliable memory characteristics, and extended data retention times. Experimental analyses of the programming and erasing behaviors under various bending conditions revealed a direct correlation between strain and charging capacity.

Additionally, the study examined the thermal-induced effects on these memory devices, noting that the mobility increased by approximately 200%, and the memory window expanded from 1.48 V to 1.8 V as the temperature increased

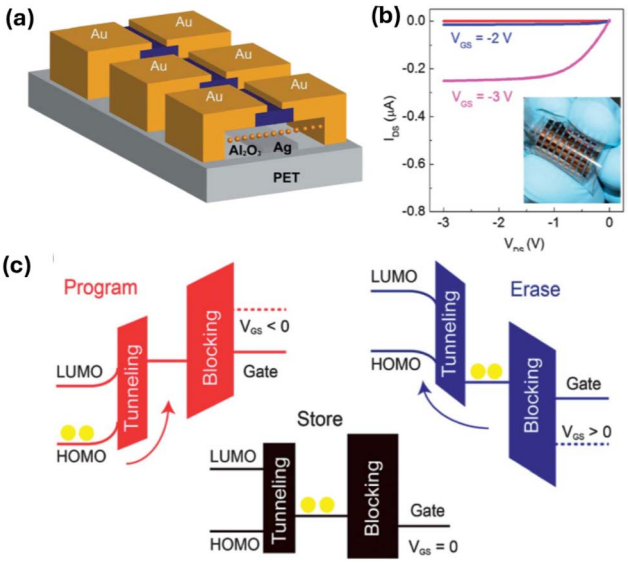

Fig. 11 Comprehensive view and characteristics of the flexible memory array. (a) Three-dimensional illustration: this panel presents a three-dimensional representation of the flexible memory array, showcasing its structural design and layout. (b) Output characteristics: the output characteristics of the memory transistors in their programmed state are displayed here. The inset provides an optical image of the flexible memory arrays, giving a visual confirmation of their physical appearance and flexibility. (c) Energy diagram: this diagram illustrates the energy levels and electron flow within the memory transistor, detailing the charge trapping and release mechanisms that underpin its operation. Reproduced from ref. 49 with permission from [RSC Publishing], copyright [2013].

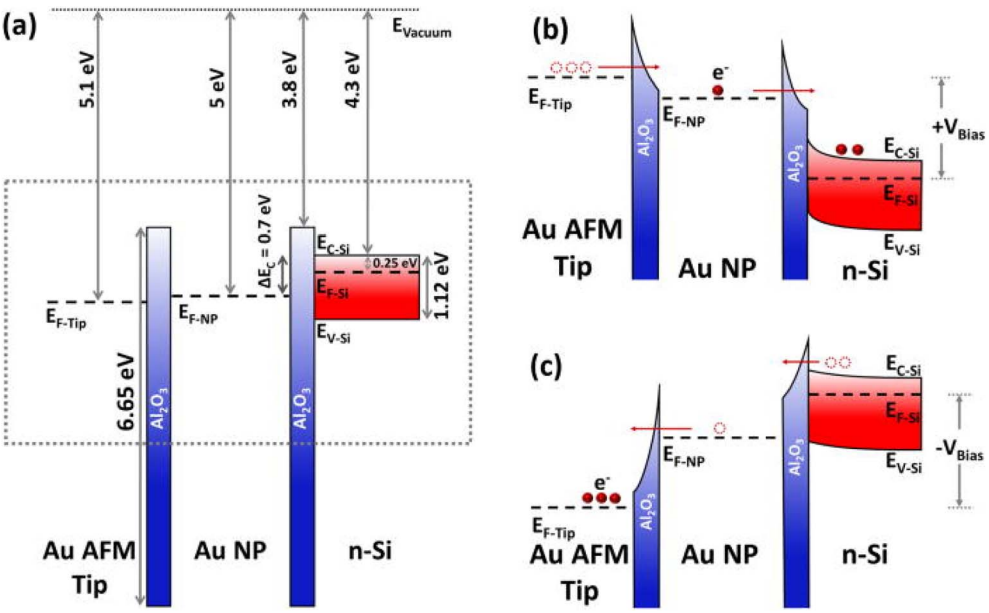

Fig. 10 Energy band diagram for NP-based memory operations: (a) energy levels of materials at zero bias, with no contacts and no charge in the Au-NP. (b) Electron energy levels during charge injection into the Au-NP under positive bias. (c) Electron energy levels during discharge of the Au-NP under negative bias. Diagrams (b) and (c) correspond to the dashed rectangle in (a). Reproduced from ref. 47 with permission from [AIP Publishing], copyright [2020].

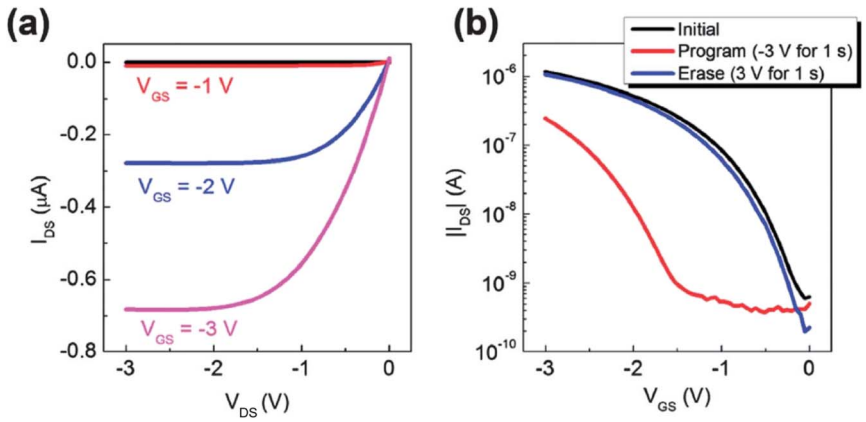

Fig. 12 (a and b) Transfer characteristics of memory arrays under different strain conditions. Reproduced from ref. 49 with permission from [RSC Publishing], copyright [2013].

from 20 °C to 80 °C. Fig. 12 shows the schematic illustrations and transfer characteristics of memory arrays under different strain conditions. This improvement is attributed to thermally activated charge transport. However, it was observed that the retention capability of the devices diminished with rising temperatures. These findings enhance our understanding of the performance of flexible organic memory transistors under diverse operational temperatures, highlighting their potential applications in temperature sensors, temperature memory devices, and advanced electronic circuits. Moreover, the low-temperature processing techniques employed for creating the Au-NP monolayer and the Al_2O_3 dielectric layer suggest that these elements could be seamlessly integrated into large-area flexible electronics. This study not only validates the applicability of such memory devices in various fields but also underscores the feasibility of incorporating them into flexible, large-scale electronic systems.

Su-Ting Han *et al.*[50] introduced a straightforward technique for fabricating microcontact printable Au-NPs charge trapping layers with exceptionally high density, intended for application in flash memory on flexible polyethylene terephthalate (PET) substrates. The method involved embedding a densely packed monolayer of Au-NPs at the interface between 200 nanometer (blocking layer) and 10 nanometer (tunneling layer) atomic layer-deposited Al_2O_3, enabling controlled multilevel data storage through external gate bias manipulation. In comparison to two reference memory devices featuring a floating gate fabricated *via* thermal evaporation and electrostatic self-assembly, the proposed approach yielded remarkable results. It achieved the largest memory window (16.5 volts) and comparatively prolonged retention time (10^5 seconds) attributable to the abundant density of storage sites and minimal lateral charge leakage. Fig. 13 displays the following: (a) Transmission Electron Microscopy (TEM) image showcasing 10 nm Au-NPs coated with dichlorodiphenyltrichloroethane (DDT). (b) UV-visible absorption spectra of Au NPs dispersed in toluene. (c) Schematic illustration detailing the process of forming an NPs array on a substrate. (d) Three-dimensional schematic representation of the memory device architecture. (e) Optical photograph capturing the fabricated flexible memory device. These findings underscore the significant potential for integrating these devices into flash memory device scaling efforts. Additionally, the memory device demonstrated robust endurance properties (exceeding 1000 cycles) and mechanical stability (over 500 bending cycles). Crucially, the method is compatible with low-temperature processing, facilitating its extension for the fabrication of large-area printed memories, thereby opening avenues for scalable and flexible memory technologies.

On the other hand, floating-gate-based flash memory faces significant limitations with continuous device scaling, due to issues such as increasing cell-to-cell interference, decreasing coupling ratios, non-scalable tunneling oxide thickness, and reduced tolerance for charge loss. As a result, active research has been directed towards flash memory devices with discrete charge trapping layers, such as silicon–oxide–nitride–oxide–silicon (SONOS) devices and nanocrystal (NC)-based memory devices, also known as nano-floating gate memory devices. These technologies have garnered interest in the electronics industry due to their superior endurance, smaller chip size, and lower power consumption compared to traditional floating-gate devices. For instance, Samsung Electronics has successfully fabricated a 64 gigabit density SONOS-type flash memory device using Si_3N_4 as the charge trapping layer. Despite this achievement, controlling the trap density and distribution in SONOS devices remains challenging. These parameters are crucial in determining the memory characteristics, particularly regarding the programmed/erased bit distribution and data retention. The variability in these factors can lead to issues with uniformity and reliability, which are critical for high-density memory applications.

In contrast, NC memory devices using semiconducting or metallic nanocrystals offer a significant advantage in controlling trap density and distribution. This control is achievable by adjusting the process parameters during synthesis, allowing for more precise engineering of the memory device characteristics. Consequently, considerable research has focused on the controlled synthesis of semiconducting or metallic

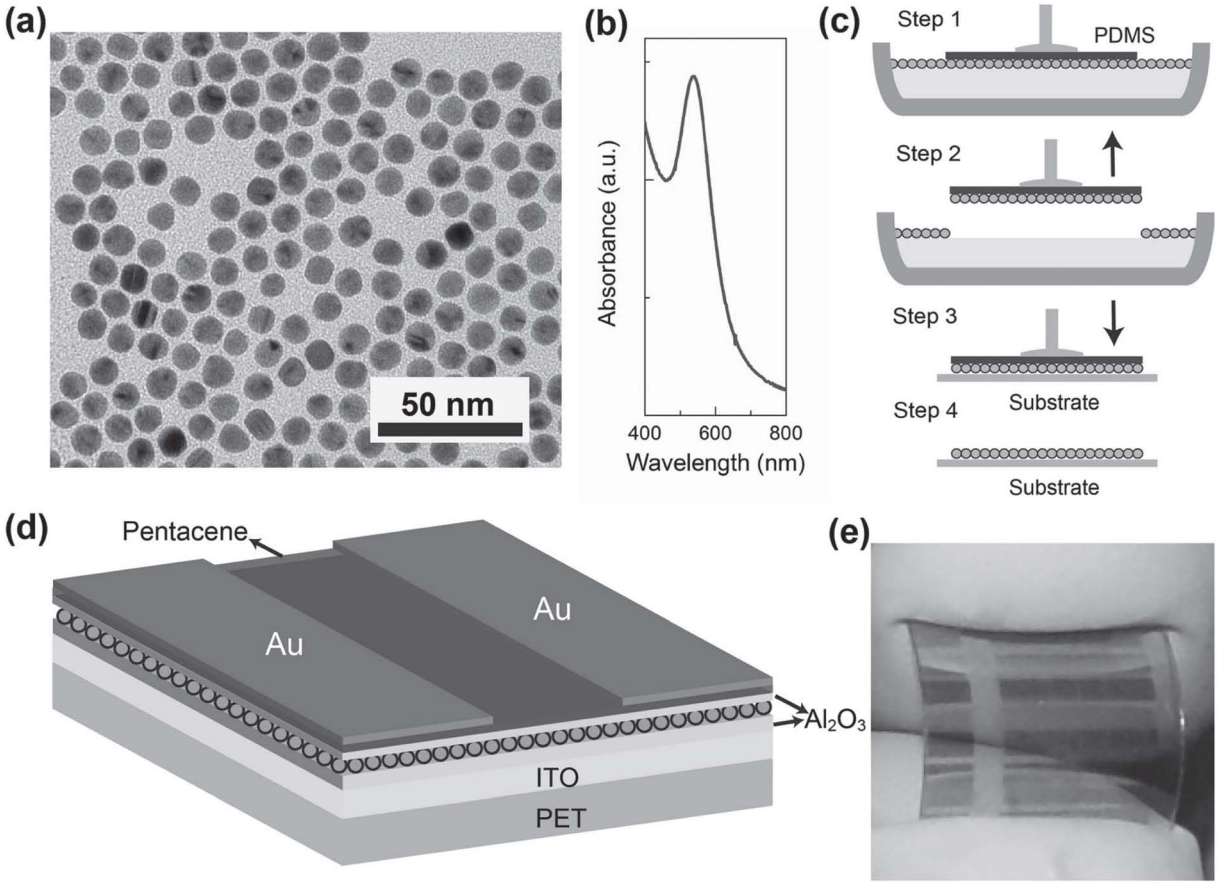

Fig. 13 Presents: (a) TEM image of 10 nm Au NPs coated with DDT. (b) UV-visible absorption spectra of Au-NPs in toluene. (c) Schematic process of forming NPs array on a substrate. (d) 3D schematic of the memory device architecture. (e) Optical photo of the fabricated flexible memory device. Reproduced from ref. 50 with permission from [Wiley], copyright [2012].

nanoparticles for non-volatile memory applications. Researchers have developed various methods to synthesize nanocrystals with controlled size, distribution, and composition, which directly influence the electrical properties and performance of the memory devices. Recently, there have been numerous reports on the fabrication of NC-based memory devices utilizing gold nanoparticles. Au-NPs are particularly attractive for these applications due to their excellent chemical stability, high electrical conductivity, and compatibility with existing semiconductor fabrication processes.

Soo-Jin Kim *et al.*[51] reported the development of controlled Au-NP based nonvolatile memory devices utilizing pentacene organic transistors and PMMA insulator layers. The memory device configuration, n^+Si gate/SiO_2, included a blocking oxide layer, polyelectrolytes, a tunneling dielectric layer, and Au source-drain electrodes. These devices demonstrated excellent programmable memory characteristics, including a notably large memory window during programming and erasing operations. Fig. 14a shows the schematic device structure: this panel illustrates the typical bottom-gate and top-contact configuration of organic transistor-based nano-floating-gate memory devices. The schematic shows the layout of the various layers, including the organic semiconductor, dielectric layers, and the nano-floating-gate layer, providing a clear depiction of the device architecture. Fig. 14b shows the program/erase characteristics: this graph presents the program and erase characteristics of the fabricated memory devices, demonstrating their ability to store and erase data efficiently. The figure highlights key performance metrics such as threshold voltage shifts, which indicate the success of programming and erasing operations. Reliability was further confirmed through data retention tests, indicating robust performance over time. The fabrication of the charge trapping and tunneling layers employed straightforward solution-based processes, specifically dipping and spin-coating techniques. Notably, the maximum processing temperature was kept below 100 °C, making this method highly suitable for applications in plastic and flexible electronics. This approach highlights the potential for integrating advanced memory devices into next-generation flexible and wearable electronic systems.

These memory devices have demonstrated enhanced performance, including improved data retention, faster programming and erasing speeds, and lower power consumption. Furthermore, NC-based memory devices are also being explored for their potential in 3D memory architectures. 3D memory stacking can significantly increase storage density and

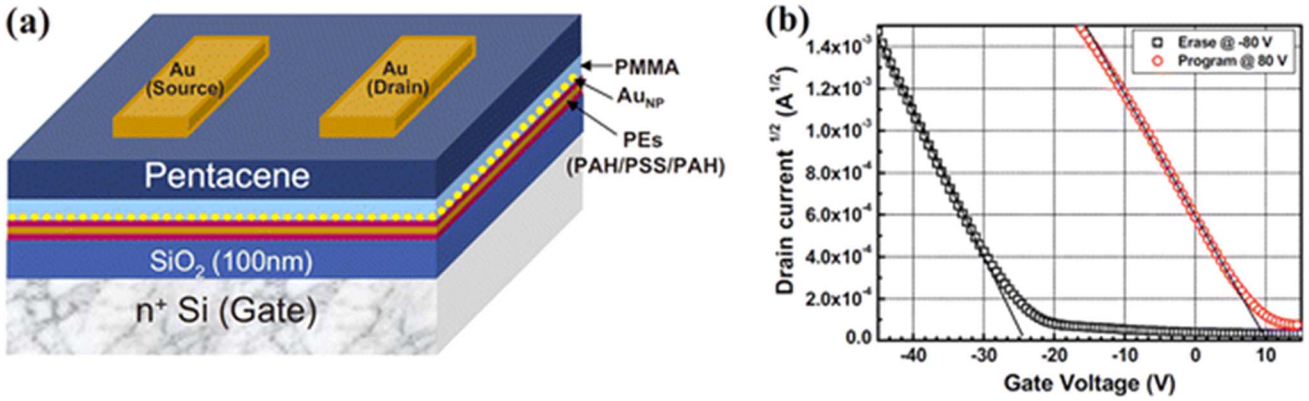

Fig. 14 (a) Device structure and (b) program/erase characteristics of organic transistor-based nano-floating-gate memory devices. Reproduced from ref. 51 with permission from [AIP Publishing], copyright [2010].

improve performance without a corresponding increase in the footprint of the memory chip. The ability to precisely control the placement and density of nanocrystals is crucial for the successful implementation of 3D memory technologies, making NC-based approaches highly promising. The advancements in NC-based memory technology also open up possibilities for integrating these devices into flexible and wearable electronics. The flexibility and mechanical robustness of nanocrystal-based memory devices make them suitable for applications in emerging technologies, such as flexible displays, wearable health monitors, and other portable electronic devices.[52–58] The ability to fabricate memory devices on flexible substrates without compromising performance is a significant step forward in the development of next-generation electronic devices. In conclusion, while floating-gate-based flash memory faces several challenges with scaling, NC-based memory devices offer a promising alternative with better control over trap density and distribution, improved performance characteristics, and potential for integration into advanced applications. Ongoing research and development in this area continue to push the boundaries of what is possible in non-volatile memory technology, paving the way for more efficient, reliable, and versatile memory solutions in the future.

6.2. Electrocatalysis

Redox enzymes present sustainable alternatives to noble metal or inorganic catalysts, particularly in electrocatalytic-based devices. However, before these biodevices can be commercially viable, several significant challenges must be addressed. These include ensuring long-term stability and managing the costs associated with enzyme production, which necessitate fundamental studies of enzyme behavior at electrochemical interfaces. Over the past two decades, considerable progress has been made in developing interfaces capable of enhancing catalytic currents and bioelectrode stability. Redox enzymes, such as bilirubin oxidases (BOD) and laccase (LAC), have been extensively studied for applications involving the oxygen reduction reaction. Despite advancements, further optimization is required to understand the relationships between enzyme orientation, conformation, loading, and electroactivity. A particularly intriguing question is the impact of enzyme–enzyme neighboring interactions on electrocatalysis, a phenomenon observed *in vivo* where protein crowding minimizes deformation to unfolded states.

Previous research has highlighted that full coverage of bilirubin oxidase on gold electrodes does not necessarily result in higher specific activity, demonstrating the intricate link between electroactivity and enzyme surface coverage. Optimum enzyme surface coverage, as demonstrated by McArdle *et al.*,[59] is crucial, as excessive coverage can lead to decreased activity. Processes such as the rigidification of proteins and their aggregation on electrode surfaces, often overlooked, may significantly influence the percentage of electroactive enzymes and should be considered in bioelectrode design and optimization efforts. One effective strategy to regulate and adjust enzyme surface coverage involves utilizing patterned surfaces with specific enzyme immobilization. These surfaces can be achieved through the formation of mixed self-assembled monolayers (SAMs) composed, for instance, of thiols carrying different functionalities. However, a challenge arises in effectively partitioning the thiol functions on the surface to achieve the desired enzyme coverage. Another widely adopted approach is the controlled assembly of particles on electrode surfaces, serving as functional units for modifying the electrode surfaces for enzyme immobilization. These particles may originate from biological sources, such as bacteriophage particles and DNA origami scaffolds, which have been patterned on gold electrodes to investigate their impact on bio electrocatalysis. Alternatively, metallic particles, particularly Au-NPs, are commonly used. Numerous studies in the literature have reported enhanced bio electrocatalytic oxygen reduction through the immobilization of enzymes like LAC and BOD on electrodes modified with various Au-NPs. Despite these advancements, there are limited reports on patterned electrodes based on Au-NPs aimed at controlling and varying enzyme coverage for bio electrocatalysis. However, recent studies have explored novel approaches such as utilizing nanosecond laser-treated and heat-sintered gold films for applications like ascorbate sensing

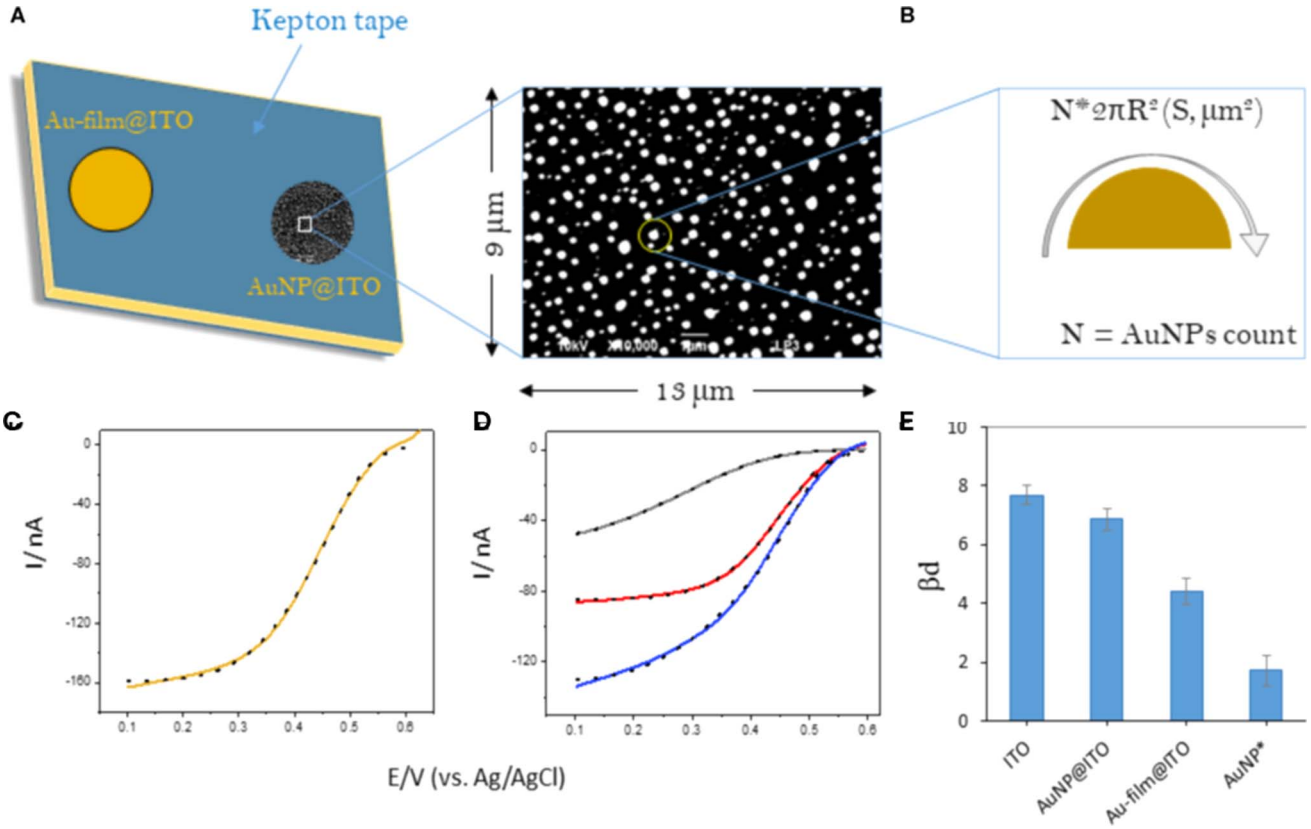

Fig. 15 Au-film@ITO or AuNP@ITO electrode setup and its electrochemical behavior: (A) the electrode configuration, highlighting the electro-accessible surface area defined by the Kepton mask. (B) A typical SEM image with dimensions provides visual insight into the electrode structure. (C and D) Electrochemical modeling is overlaid on corresponding cyclic voltammograms (CVs). (E) The graph displays changes in bd upon *Myrothecium verrucaria* bilirubin oxidase (*Mv* BOD) adsorption. Reproduced from ref. 60 with permission from [Frontiers], copyright [2020].

and enzymatic glucose oxidation. Particularly, the latter work emphasized the critical role of inter-enzyme agglomeration in bio electrocatalysis and proposed spatial control of enzyme immobilization as a means to overcome this challenge. These innovative techniques offer promising avenues for advancing the field of bio electrocatalysis and developing more efficient enzyme-based electrochemical devices.

Vivek Pratap Hitaishi and colleagues[60] explored the interaction between nanosecond laser pulses and nanometric gold films deposited on indium tin oxide (ITO) substrates, resulting in the *in situ* generation of gold nanoparticles (Au-NP@ITO). The study delves into the influence of various parameters such as gold film thickness, laser energy, interaction time scale, and pulse characteristics on the formation of nanoparticles. A comprehensive analysis of Au-NP size, coverage, and the ratio of total surface area to electroactive surface area is provided, correlating these factors with the thickness of the treated gold layer. Fig. 15 illustrates key aspects of the Au-film@ITO or Au-NP@ITO electrode setup and its electrochemical behavior. Utilizing microscopy techniques alongside electrochemical analyses, the research showcases the long-term stability of AuNP@ITO electrodes under atmospheric conditions and in electrolytic environments. Furthermore, the study evaluates the adsorption of enzymes and subsequent bio electrocatalytic activities following specific chemical modifications of the Au-NPs. Of particular focus are two multicopper enzymes (MCOs), namely, *Myrothecium verrucaria* BOD and *Thermus thermophilus* LAC, chosen to demonstrate the efficacy of AuNP@ITO electrodes in bio electrocatalysis applications.

6.3. Electrochemical

The utilization of metal nanoparticles thin films at electrode/solution interfaces has emerged as a promising strategy for functionalizing electrode surfaces and constructing nanoscale devices. Among these nanoparticles, Au-NPs monolayers stand out due to their unique properties, including high chemical stability, biocompatibility, and their ability to bind amine/thiol terminal groups of organic molecules. These characteristics make Au-NPs highly attractive for a range of electrochemical applications, including sensors, biosensors, and energy storage systems. Several studies have explored the potential of Au-NP monolayers in electrochemical applications. For instance, Tian *et al.*[61] have developed a straightforward and highly reproducible method for immobilizing Au-NP monolayers of varying sizes onto amine-terminated, activated boron-doped diamond (BDD) substrates. This study details the preparation, characterization, and electrochemical properties of BDD electrodes modified with self-assembled colloidal Au-NP layers. The method leverages the ability of Au-NPs to covalently bond with

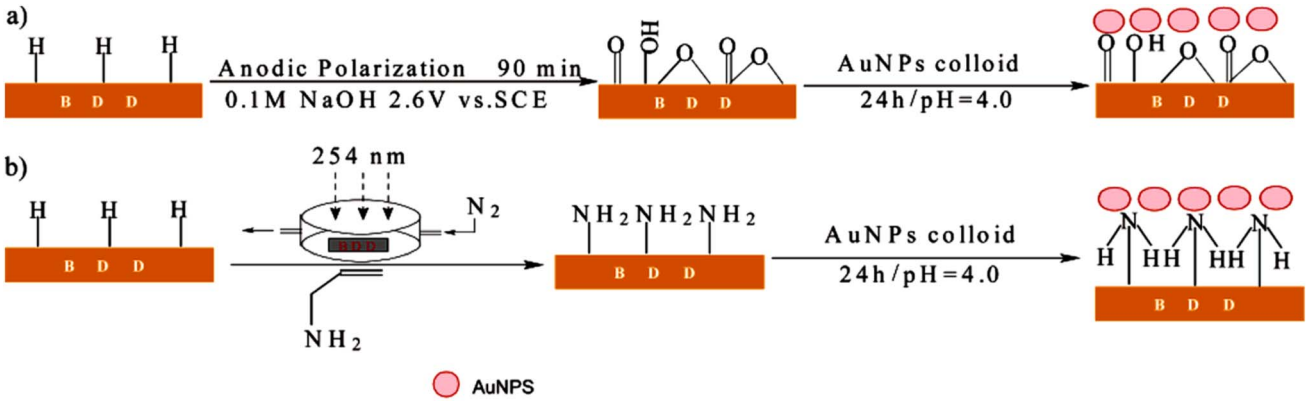

Fig. 16 The self-assembly of Au-NPs onto BDD surfaces: (a) hydroxyl/oxide-terminated activated BDD surface, and (b) amine-terminated activated BDD surface. Reproduced from ref. 61 with permission from [ACS Publications], copyright [2006].

the lone pairs of terminals $-NH_2$ groups in organic entities, with these interactions being further enhanced by electrostatic attraction between oppositely charged components. Fig. 16 illustrates the process of Au-NP self-assembly onto BDD surfaces. Initially, (a) the BDD surface is activated to produce a hydroxyl/oxide-terminated surface. Subsequently, (b) this surface is further modified to generate an amine-terminated activated BDD surface, facilitating the self-assembly of Au-NPs. Surface properties were investigated which confirmed that the Au-NP monolayers retained key characteristics of individual particles, such as size-dependent (tunable) electrochemical behavior. Notably, the study found that the electrochemical behavior of $Fe(CN)_6^{3-/4-}$ on Au-NPs-BDD electrodes became more reversible as the size of the Au-NPs decreased. Fig. 17a SEM images of amine-terminated activated BDD surfaces after exposure to Au colloidal solutions for 6 hours; AuNP sizes are approximately 15 nm. Fig. 17b presents cyclic voltammograms (CVs) of 1 mM $Fe(CN)_6^{3-/4-}$ in 0.1 M Na_2SO_4, obtained from: (a) as-grown BDD, (b) amine-terminated activated BDD, (c) BDD modified with a 15 nm Au-NPs monolayer, and (d) BDD modified with a 40 nm Au-NPs monolayer. The scan rate is 50 mV s^{-1}. This method offers a valuable approach to controlling the interfacial properties of diamond films, providing high durability and potential for developing innovative biosensor configurations and electronic devices.

Hence, the incorporation of AuNP monolayers into electrochemical systems has opened up new possibilities for the development of next-generation devices with enhanced functionality and performance. Ongoing research and innovation are expected to further expand the applications of Au-NP monolayers, paving the way for new breakthroughs in energy storage, environmental monitoring, and biomedical diagnostics.

6.4. Biosensors

6.4.1. Cholesterol biosensor. Nandi Zhou *et al.*[62] demonstrated that Au-NP seeds could be adsorbed onto the surface of a self-assembled monolayer (SAM)-modified electrode. When this modified electrode was treated with an Au-NP growth

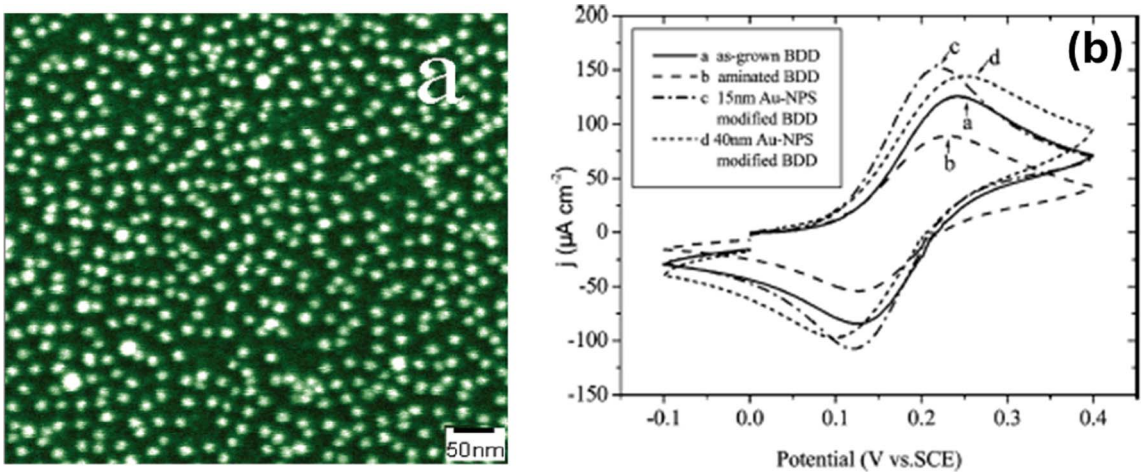

Fig. 17 (a) SEM images of amine-terminated BDD surfaces exposed to 15 nm Au-NP solutions for 6 hours. (b) CVs of 1 mM $Fe(CN)_6^{3-/4-}$ in 0.1 M Na_2SO_4 at 50 mV s^{-1} for (a) as-grown BDD, (b) amine-terminated BDD, (c) 15 nm Au-NPs on BDD, and (d) 40 nm Au-NPs on BDD. Reproduced from ref. 61 with permission from [ACS Publications], copyright [2006].

solution containing various concentrations of H_2O_2 or cholesterol along with cholesterol oxidase (ChO_x), the Au-NP seeds on the electrode surface enlarged to various degrees. Consequently, the peak currents in the cyclic voltammograms were inversely proportional to the concentration of H_2O_2 or cholesterol. Furthermore, ChO_x was modified onto the surface of the Au/SAM/Au-NP electrode, creating an Au/SAM/Au-NP/ChO_x electrode. This enzyme-modified electrode, used for cholesterol detection, achieved an exceptionally low detection limit of 5×10^{-9} M, with two linear dependence ranges of 7.5×10^{-8} to 1×10^{-6} and 1×10^{-6} to 5×10^{-5} M. Additionally, it has been reported that not only H_2O_2 but also NADH (NADPH), reduced FAD-dependent enzymes with appropriate mediators, and even some small active molecules can mediate the enlargement of Au-NPs. Therefore, the sensor model introduced in this research has potential applications across a broad range of fields. This method could revolutionize the design and functionality of biosensors, making them more versatile and efficient for detecting a wide array of biochemical substances.

6.4.2. Enzyme biosensor. Byung-Wook Park *et al.*[63] reported the development of an enzyme biosensor matrix by modifying the surface of a gold electrode with Au-NPs and mixed self-assembled monolayers (SAMs). Horseradish peroxidase (HRP) was immobilized on this modified surface to create a biosensor. The study compared the Au-NP modified gold electrode and a bare gold electrode in terms of surface area and electric current using AFM and cyclic voltammetry (CV). The Au-NPs adhered strongly to the gold electrode surface, showed uniform distribution, and demonstrated high stability. A mixed SAM was formed using dithiobis-*N*-succinimidyl propionate (DTSP) and inert tetradecane-1-thiol (TDT) through a reductive desorption technique. Fig. 18 shows the enzyme immobilization methods: (a) SAM (Self-Assembled Monolayer): enzymes are immobilized *via* a covalently bonded monolayer formed on the electrode surface. (b) Direct adsorption: enzymes adhere directly to the electrode surface through physical interactions. (c) Polymer gel entrapment: enzymes are enclosed within a polymer gel matrix applied to the electrode surface, offering stability and protection. Cyclic voltammetry was used to verify the formation of this mixed deposition. Initially, 3-mercaptopropionic acid (MPA) and TDT were deposited at specific ratios, followed by the desorption of MPA *via* electric potential application. DTSP was then deposited in the areas where MPA had been desorbed. The study examined ratios of 20 : 80 and 50 : 50 between MPA and TDT and discussed the differences in CV responses. HRP immobilization on the mixed SAM surface provided an effective method for stable enzyme attachment. The presence of AuNPs enhanced electrochemical activity, requiring minimal amounts of samples and enzymes while preventing enzyme leakage due to the SAM matrix. Notably, the mixed SAM exhibited unique CV characteristics compared to single-molecule SAMs. The reaction kinetics of the SAM-immobilized enzyme followed the Michaelis–Menten equation. The Michaelis–Menten reaction rate equation is given by:

$$I = \{I_{max}[C]\}/\{K_m + [C]\} \quad (9)$$

where (I) is the current measured, ($I_{\{max\}}$) is the maximum current at substrate saturation, (C) is the substrate concentration, and (K_m) is the Michaelis constant. Kinetic parameters were derived from the Lineweaver–Burke plot:

$$\{1\}/\{I_{ss}\} = \{K_m\}/\{I_{max}\,[C]\} + \{1\}/\{I_{max}\} \quad (10)$$

By plotting $1/C$ *versus* $1/I_{ss}$, K_m and I_{max} were determined to be 16.7 μM and 833.33 nA, respectively. The low Michaelis constant suggests minimal diffusion limitations within the AuNP-modified electrode, and the high I_{max} indicates a significant number of immobilized enzymes. This study highlights the importance of diffusion barriers commonly encountered in enzyme-entrapped electrode matrices and demonstrates the beneficial measurement of K_m and I_{max} values for the enzyme biosensor.

6.4.3. Immunological biosensor. Mehmet Cetin Canbaz *et al.*[64] have introduced a novel immunological biosensor designed for highly sensitive quantification of human epidermal growth factor receptor-3 (HER-3). The biosensor was constructed by sequentially layering the gold electrode surface with hexanedithiol, gold nanoparticles, and cysteamine. Through covalent attachment facilitated by glutaraldehyde, anti-HER-3 antibody was immobilized onto cysteamine, serving as the bioreceptor in this biosensor setup, a pioneering approach in biosensor technology. Surface characterization was conducted using electrochemical impedance spectroscopy and voltammetry, revealing promising analytical performance in detecting HER-3 concentrations ranging from 0.2 to 1.4 pg mL^{-1}. Additionally, the experimental impedance data underwent Kramers–Kronig transform for further analysis. Notably, the single frequency impedance technique was employed for the first time to characterize the interaction between HER-3 and anti-HER-3 in an immunosensor system. This innovative approach enables continuous and rapid measurements, offering a cost-effective solution with the use of a simple potentiostat. The biosensor was successfully tested on artificial serum samples spiked with HER-3, demonstrating its potential for practical applications in biosensing. This study underscores the versatility of single frequency impedance for various biosensor applications, including monitoring and elucidating

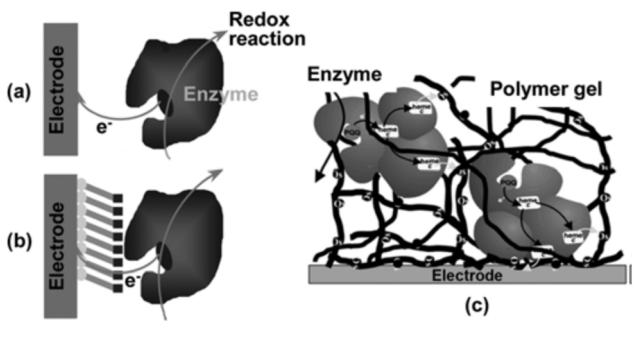

Fig. 18 Enzyme immobilization methods: (a) SAM, (b) direct adsorption, and (c) polymer gel entrapment. Reproduced from ref. 63 with permission from [Springer Nature], copyright [2010].

slow time-dependent changes on biosensor surfaces, thus advocating for its wider adoption in biosensor research and development.[65]

6.4.4. Amperometric acetylcholinesterase (AchE) biosensors. Amperometric enzymatic biosensors have emerged as highly suitable tools for biochemical analysis, offering notable attributes such as selectivity, sensitivity, rapid response, compact size, and reproducibility. The amalgamation of enzymatic reactions with electrochemical methods has paved the way for various enzyme-based electrochemical biosensors, enabling sensitive and swift determination in environmental analyses. Particularly, amperometric acetylcholinesterase (AChE) biosensors have demonstrated efficacy in pesticide analysis by detecting AChE inhibition, wherein enzymatic activity serves as a gauge for pesticide quantification. A primary challenge in developing sensitive and robust biosensors lies in effectively immobilizing enzymes onto solid electrode surfaces. Direct adsorption of enzymes onto bare gold surfaces often leads to denaturation and loss of bioactivity. SAMs of alkanethiols on gold substrates offer a straightforward approach to creating well-defined surfaces with controllable chemical functionality, serving as a foundation for surface modification. These SAMs, when terminated with carboxylic groups, facilitate further functionalization using carbodiimide chemistry for biomolecule attachment, such as proteins, DNA, and antibodies. SAMs act as barriers, preventing proteins and ligands from contacting the metal surface. These stable, densely packed SAMs on gold electrodes typically exhibit minimal defects and high resistance to ion penetration, which may hinder electron transfer between the electrode surface and electroactive species in solution. To address these electron transfer challenges, incorporating metal nanoparticles becomes essential. Metal nanoparticles, including Au-NPs, offer benefits such as roughening the conductive sensing interface, catalytic properties, and enhanced conductivity. Au-NPs, in particular, have gained widespread use in fabricating electrochemical biosensors. Electrochemical deposition stands out as a simple and moderate method for Au-NP fabrication, enabling selective film deposition with controllable thickness. This electrochemical approach provides a swift and straightforward alternative for preparing Au-NP modified electrodes, facilitating rapid biosensor development.

Dan Du *et al.*[66] developed a comprehensive methodology for the synthesis and functionalization of AuNPs on Au substrates, optimizing each step for enhanced stability and biomolecule immobilization efficiency. The *in situ* synthesis of Au-NPs allowed for precise control over their size and distribution, ensuring uniform coverage on the substrate surface. This facilitated electron transfer across the SAMs, enhancing the overall performance of the biosensor. Characterization techniques such as contact angle measurement, cyclic voltammetry, and electrochemical impedance spectroscopy provided detailed insights into the surface properties and functionality of the modified interface. Fig. 19a illustrates the principle of utilizing Au-NPs as mediators for electron transfer across SAMs in the design of AChE biosensors. The immobilization of AChE as a model enzyme demonstrated excellent activity towards its substrate, underscoring the efficacy of the biosensor design. The stability of the AChE biosensor under optimal conditions was particularly noteworthy, indicating the robustness of the

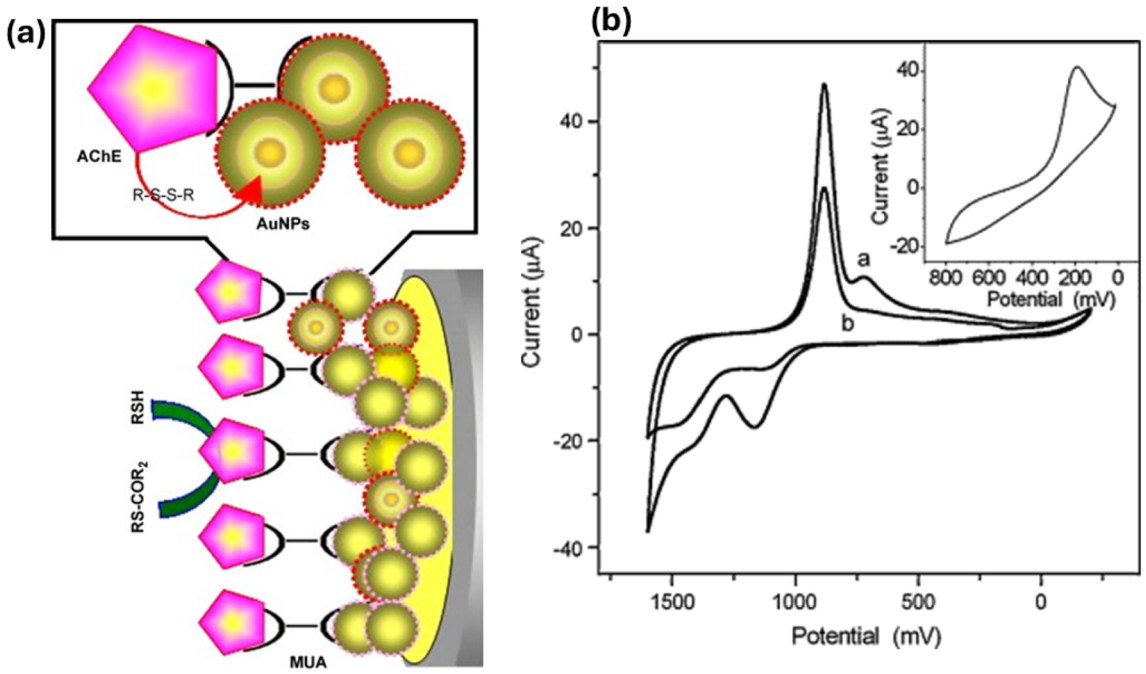

Fig. 19 (a) Principle of Au-NPs acting as a mediator for electron transfer across SAMs in the design of an AChE biosensor. (b) Cyclic voltammograms obtained from Au-NPs/Au (a) and bare Au (b) in 0.5 M H_2SO_4. The inset shows cyclic voltammograms of 0.1% $HAuCl_4 \cdot 4H_2O$ reduction. Reproduced from ref. 66 with permission from [Elsevier], copyright [2008].

immobilization strategy. Furthermore, the biosensor exhibited a wide dynamic range for the detection of malathion, a commonly encountered pesticide, with a low detection limit: 0.001 to 0.1 μg mL^{-1} and 0.1 to 25 μg mL^{-1}, with a detection limit of 0.001 μg mL^{-1}, highlighting its potential for environmental monitoring and pesticide residue analysis. Fig. 19b compares cyclic voltammograms of Au-NPs/Au (a) and bare Au (b) in 0.5 M H_2SO_4. Inset shows cyclic voltammograms of 0.1% $HAuCl_4 \cdot 4H_2O$ reduction. The simplicity and reproducibility of the developed method make it suitable for scalable biosensor fabrication, offering promising avenues for widespread deployment in analytical laboratories and field applications. Additionally, the versatility of the approach opens up possibilities for the design of biosensors targeting various analytes beyond malathion, addressing diverse environmental and biomedical challenges. Further research may focus on exploring the applicability of this biosensor platform in real-world scenarios and optimizing its performance for specific analytical requirements.

M. L. Mena *et al.*[67] conducted a comparative study on the analytical performance of various enzyme biosensor designs, specifically focusing on different gold nanoparticle-modified electrode surfaces. These biosensors utilized glucose oxidase (GO_x) and the redox mediator tetrathiafulvalene, coimmobilized through crosslinking with glutaraldehyde. The designs tested included: (i) colloidal gold (Au_{coll}) bound to cysteamine (Cyst) monolayers self-assembled on a gold disk electrode (Au-E) and (ii) glassy carbon electrodes (GCEs) modified with electrodeposited gold nanoparticles (nAu). The performance of these designs was compared with biosensors comprising GO_x immobilized on Cyst-modified AuE (GO_x/Cyst–AuE) and mercaptopropionic acid-modified AuE (GO_x/MPA–AuE). Fig. 20. Schemes displaying the strategies for the preparation of glucose oxidase biosensor designs using different tailored gold nanoparticle-modified electrode surfaces: (A) GO_x/Au_{coll}–Cyst–AuE: Glucose oxidase (GO_x) immobilized on colloidal gold (Au_{coll}) bound to a cysteamine (Cyst) self-assembled monolayer on a gold disk electrode (AuE). (B) GO_x/Au_{coll}–Cyst/Cyst–AuE:

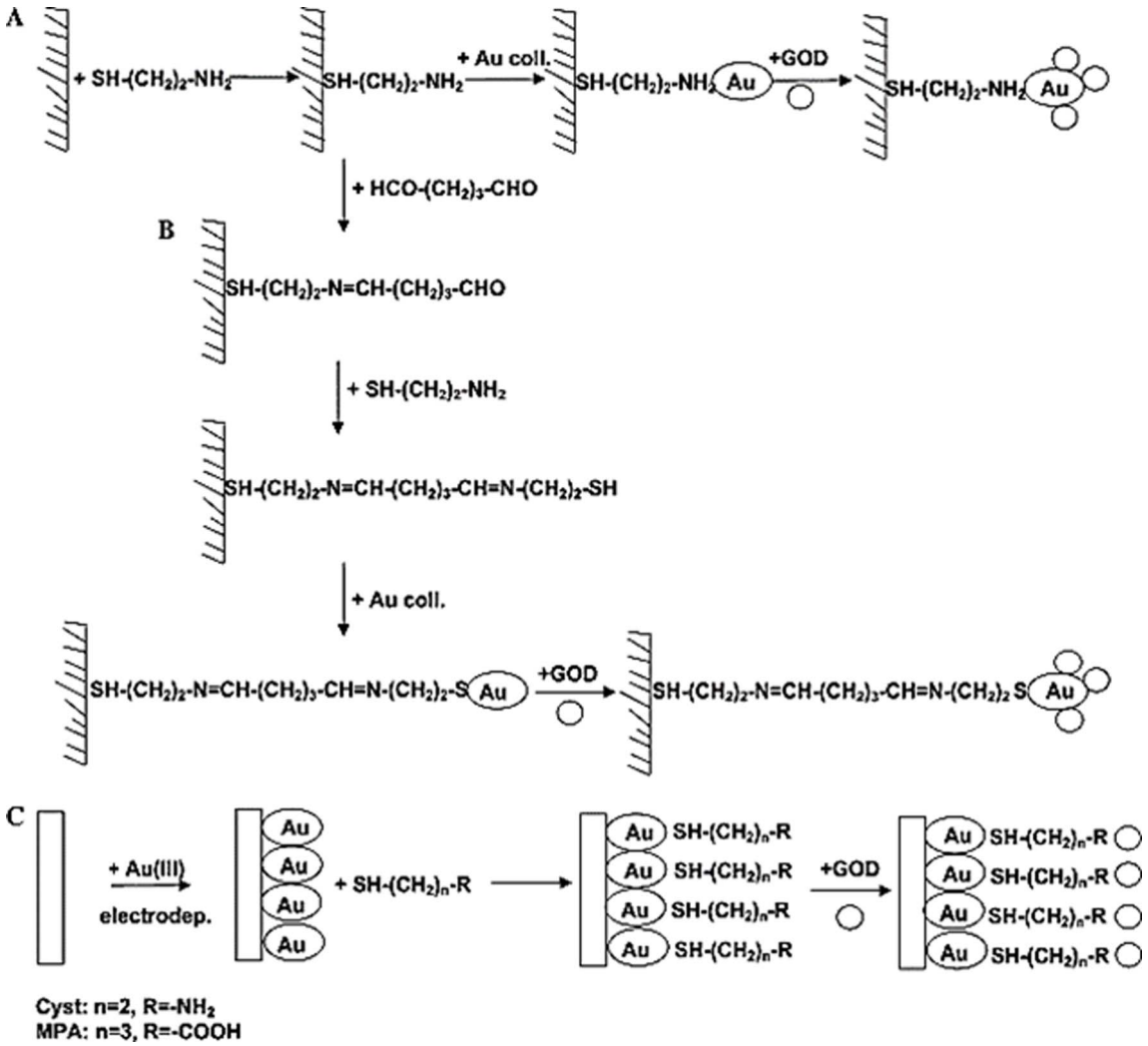

Fig. 20 Preparation strategies for glucose oxidase biosensors using gold nanoparticle-modified electrodes: (A) GO_x/Au_{coll}–Cyst–AuE, (B) GO_x/Au_{coll}–Cyst/Cyst–AuE, (C) GO_x/Cyst–nAu–GCE or GO_x/MPA–nAu–GCE. Reproduced from ref. 67 with permission from [Elsevier], copyright [2005].

GO_x immobilized on colloidal gold (Au_{coll}) bound to a double layer of cysteamine (Cyst) self-assembled monolayers on a gold disk electrode (AuE). (C) GO_x/Cyst–nAu–GCE or GO_x/MPA–nAu–GCE: GO_x immobilized on gold nanoparticles (nAu) electrodeposited on a glassy carbon electrode (GCE), with either cysteamine (Cyst) or mercaptopropionic acid (MPA) self-assembled monolayers. For the second design approach, configurations included direct immobilization of GO_x on nAu-modified GCE (GO_x/nAu–GCE), and on Cyst or MPA SAMs bound to gold nanoparticles (GO_x/Cyst–nAu–GCE or GO_x/MPA–nAu–GCE, respectively). Analytical characteristics of glucose calibration plots and kinetic parameters of enzyme reactions were evaluated for all biosensors. The GO_x/Au_{coll}–Cyst–AuE design demonstrated higher sensitivity for glucose determination than GO_x/Cyst–AuE and GO_x/Au_{coll}–Cyst/Cyst–AuE, and similar sensitivity to GO_x/MPA–AuE. Furthermore, the GO_x/Au_{coll}–Cyst–AuE biosensor exhibited a notably longer useful lifetime of 28 days, significantly surpassing the other GO_x biosensor designs. This study highlights the impact of gold nanoparticle modification on enhancing the performance and longevity of enzyme biosensors.

Fabiana Arduini *et al.*[68] developed a mono-enzymatic AChE amperometric biosensor aimed at detecting organophosphate compounds. The biosensor was constructed by immobilizing the AChE enzyme using glutaraldehyde on a preformed cysteamine SAM on gold-screen printed electrodes (Au-SPEs). Fig. 21 shows a schematic of the assembly of the AChE biosensor. Enzymatic activity was monitored by measuring the product, thiocholine, at an applied potential of +400 mV *vs.* Ag/AgCl, using ferricyanide as an electrochemical mediator. The electrocatalytic activity of ferricyanide towards thiocholine was investigated using the Nicholson–Shain method, revealing a second-order homogeneous rate constant (k_s) of $((5.26 \pm 0.65) \times 10^4)$ M^{-1} s^{-1}. To optimize the sensitivity of the biosensor, various parameters were adjusted, including the concentration of cysteamine, the duration of SAM deposition, and the concentration of AChE. Using paraoxon as a model compound, the biosensor demonstrated a linear detection range up to 40 parts per billion (ppb) with a detection limit of 2 ppb, corresponding to 10% inhibition. The effectiveness of the biosensor was validated using drinking water samples, indicating its potential as a practical analytical tool for detecting organophosphorus insecticides.

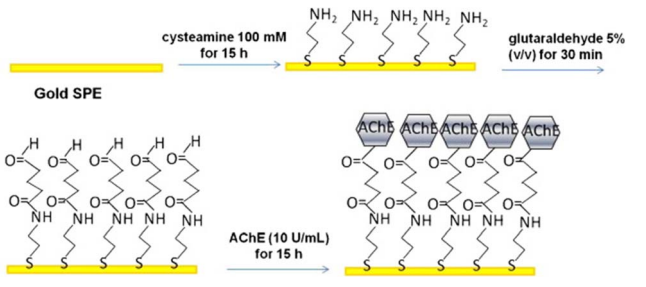

Fig. 21 Assembly process of the AChE biosensor. Reproduced from ref. 68 with permission from [Elsevier], copyright [2013].

6.4.5. DNA electrochemical biosensor. In recent years, DNA electrochemical biosensors have garnered significant attention for their sensitive, accurate, and cost-effective applications in various fields such as medical diagnostics, clinical genetics, forensics, and environmental monitoring. The key challenge in developing these biosensors lies in achieving stable immobilization of probe single-stranded DNA (ssDNA) and ensuring accessibility of the target DNA to the immobilized probe DNA on the electrode surface. The amount and molecular orientation of the immobilized probe ssDNA significantly impacts the biosensor's performance. To address this challenge, various immobilization strategies have been proposed, aiming to improve the stability of the DNA-transducer surface linkage, increase the amount of immobilized DNA, and simplify the immobilization procedure. Au-NPs have emerged as a versatile nanomaterial for enhancing the performance of DNA or protein biosensors. Self-assembly of Au-NPs on electrode surfaces can be achieved using bi-functional chemical linking agents like 1,6-hexanedithiol or cysteamine. However, these methods often result in insulated monolayers on the electrode surface, hindering efficient electron transfer between Au-NPs and the electrode. Therefore, there is a need for novel strategies to immobilize Au-NPs effectively, ensuring good electrical conductivity and electron transfer ability in biosensor fabrication. Diazonium organic salts have been widely utilized for surface derivatization of various metal and semiconductor materials. Diazonium-functionalized electrodes offer the advantage of covalent bonding with phenolic, imidazole, or amino groups, enabling diverse surface modifications. Feng Li *et al.*[69] research proposes a novel strategy for Au-NPs assembly on electrode surfaces, followed by its application in DNA electrochemical biosensors. Fig. 22 schematically represents the fabrication processes of DNA biosensor. Initially, 4-aminothiophenol (4-ATP) is self-assembled on the gold electrode *via* an Au–S bond. Subsequent diazotization of the amine group with nitrous acid yields a mercapto-diazoaminobenzene monolayer-modified electrode. This monolayer facilitates the assembly of Au-NPs on the electrode surface *via* thiol groups, improving electron transfer ability due to its large, conjugated structure. The fabricated DNA biosensor exhibits excellent sensitivity, selectivity, and regeneration ability, as determined by differential pulse voltammetry using Co(phen)33+ as an electrochemical indicator. The biosensor demonstrates a linear detection range for complementary target DNA with a low detection limit of 9.10×10^{-11} M, offering a facile and effective approach for Au-NPs modification and DNA electrochemical biosensor fabrication.

Subramanian Balamurugan *et al.*[70] conducted a study aimed at optimizing the specificity of aptamer-based SAMs supported on gold surfaces for highly specific interactions with thrombin protein. By investigating various linkers and coadsorbents, they sought to maximize target binding while ensuring specificity. Using thrombin-binding aptamers as models, different mixed monolayer systems were compared to enhance binding and selectivity. Their findings, measured *via* surface plasmon resonance (SPR) and ellipsometry, revealed that the aptamer SAMs'

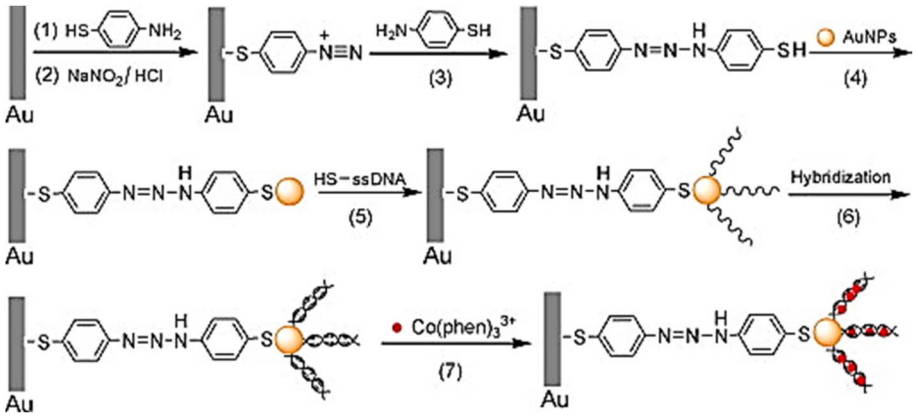

Fig. 22 Fabrication of DNA biosensor. Reproduced from ref. 69 with permission from [Elsevier], copyright [2005].

binding performance was primarily influenced by the linker, with the coadsorbent playing a secondary role. SAMs constructed with HS-$(CH_2)_6$-$OP(O)_2O$-$(CH_2CH_2O)_6$-TTTTT-aptamer exhibited a fourfold increase in binding capacity compared to those without this modification. As shown in Fig. 23, highly target-specific biosensing surfaces were created *via* aptamer monolayers on Au-NPs. Moreover, SAMs incorporating this linker demonstrated nearly complete specificity for thrombin over bovine serum albumin (BSA), indicating less than 2% non-specific binding. Interestingly, regardless of the aptamer-linker system used, the addition of HS-$(CH_2)_{11}(OCH_2CH_2)_3OH$, known as EG3, as a coadsorbent significantly enhanced thrombin binding by approximately 2.5-fold compared to HS-$(CH_2)_6$-OH (mercaptohexanol, MCH). These findings underscore the importance of linker and coadsorbent selection in optimizing the specificity and sensitivity of aptamer-based SAMs, offering valuable insights for the development of highly specific biosensing platforms.

6.4.6. Glucose biosensor. The utilization of Au-NPs in biosensors allows for enhanced sensitivity and selectivity, making them ideal for detecting various biomolecules and analytes with high precision. One of the primary benefits of Au-NPs in biosensors is their ability to facilitate efficient electron transfer, which is crucial for the accurate detection of target molecules. SAMs of Au-NPs can be tailored to possess specific functional groups that enhance the binding of enzymes, antibodies, or nucleic acids, thereby improving the biosensor's overall performance. The integration of Au-NPs with SAMs on electrode surfaces has been shown to create well-organized and stable platforms for biomolecule immobilization, which is essential for developing reliable and reproducible biosensors. The self-assembly process of Au-NPs onto electrode surfaces can be achieved through various methods, including the use of bifunctional chemical linkers, electrochemical deposition, and polymerization techniques. These methods allow for the precise control of the Au-NPs' size, distribution, and density on the

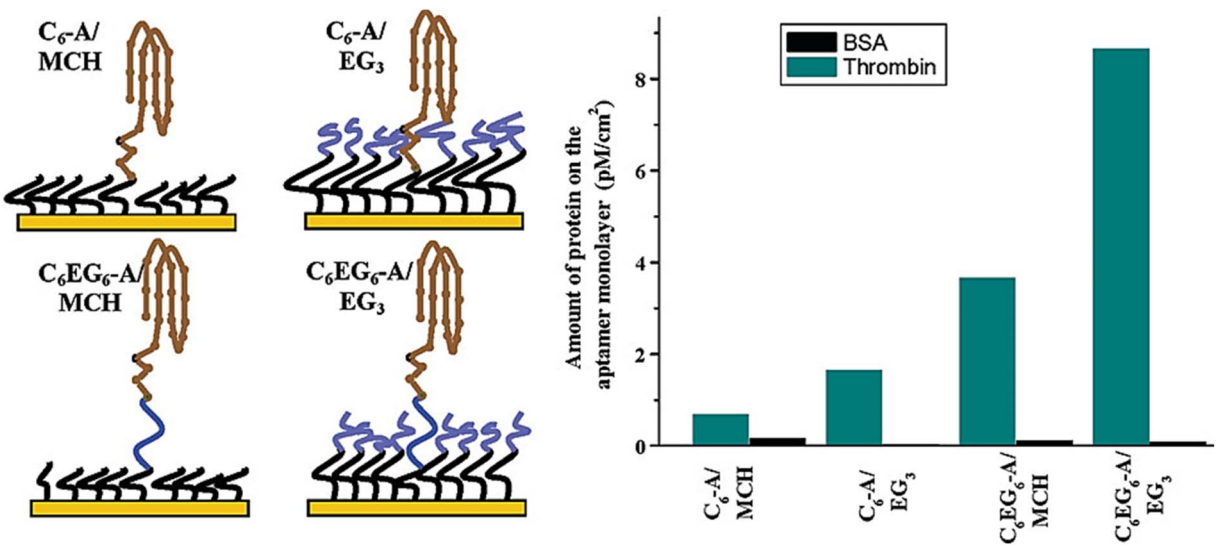

Fig. 23 Creating highly target-specific biosensing surfaces *via* aptamer monolayers on AuNPs. Reproduced from ref. 70 with permission from [Elsevier], copyright [2013].

electrode surface, which in turn influences the biosensor's analytical performance.

Xia Zhong *et al.*[71] reported the development of a novel glucose biosensor fabricated by self-assembling a double-layer 2D-network of (3-mercaptopropyl)-trimethoxysilane (MPS), gold nanoparticles, and glucose oxidase (GOD) on a gold substrate. The fabrication process involved several key steps: a clean gold electrode was immersed in an MPS solution to produce a self-assembled monolayer. Subsequently, the silane units were polymerized into a 2D-network by dipping the electrode into an aqueous NaOH solution. A second silane layer was formed by immersing the electrode back into the MPS solution overnight. Gold nanoparticles were then chemisorbed onto the thiol groups of the second silane layer, followed by the adsorption of GOD onto the surface of the gold nanoparticles. This multi-layered modification process was characterized by using electrochemical impedance spectroscopy (EIS) and cyclic voltammetry (CV), which confirmed the successful assembly and functionality of the biosensor. The analytical parameters, such as pH and temperature, were optimized to achieve the best performance. The modified electrode demonstrated an excellent electrocatalytically response to glucose in the presence of Co(byp)33+ as a mediator. The peak currents were proportional to the glucose concentration in the range of 4.00×10^{-10} to 5.28×10^{-8} M, with a correlation coefficient of 0.99, indicating high sensitivity and a broad detection range. Moreover, the modified electrode exhibited good stability and sensitivity, making it a promising tool for glucose monitoring. Overall, the integration of Au-NP monolayers in biosensor designs represents a significant advancement in the development of highly sensitive and reliable biosensors. The unique properties of Au-NPs, combined with their ease of functionalization and strong binding capabilities, make them ideal candidates for a wide range of biosensing applications, including medical diagnostics, environmental monitoring, and food safety testing.

6.4.7. Surface plasmon resonance biosensor. Au-NP monolayers have emerged as a pivotal element in the advancement of surface plasmon resonance (SPR) biosensors. These biosensors harness the unique optical properties of Au-NPs to detect biomolecular interactions with high sensitivity and specificity. SPR biosensors are widely used in various fields, including medical diagnostics, environmental monitoring, and food safety, due to their ability to provide real-time, label-free detection of analytes. SAMs of organosulfur compounds such as thiols, sulfides, and disulfides on coinage metals like copper (Cu), silver (Ag), and gold (Au) are fundamental to the construction of these biosensors. These SAMs are easy to prepare and have diverse applications, ranging from medicine to microelectronics. Grabar *et al.*[72] demonstrated that Au-NPs can form strong covalent bonds with SAMs through functional groups such as cyanide (CN), amine (NH_2), or thiol (SH). This capability is particularly useful in sensor device fabrication, where SAMs derived from thiol compounds are often used as insulators. In biosensor applications, the high selectivity of biomolecules—such as antibodies, receptors, enzymes, and nucleic acids—is crucial. These biomolecules, or capture molecules, are typically immobilized on or near the transducer surface to maintain their biological activity. Effective immobilization strategies are essential to ensure that the biological components remain functional and capable of interacting with their target analytes. Surface plasmon resonance (SPR) is extensively used to characterize the formation of monolayers or thin films on metal supports. SPR can monitor the adsorption of proteins and other biomaterials on metal surfaces, providing insights into biomolecular interactions. SPR biosensors have become indispensable for characterizing and quantifying these interactions, and their development for detecting chemical and biological species has gained significant momentum. Numerous studies have reported the use of SPR biosensors in detecting analytes pertinent to medical diagnostics, environmental monitoring, and food safety.

E. M. S. Azzam *et al.*[73] reported the fabrication of an SPR biosensor designed for the detection of the model protein bovine serum albumin (BSA). The process began with a gold substrate on which a 1,10-decanedithiol (1,10-DDT) SAM was grown. This SAM facilitated the chemisorption of Au-NPs, to which the protein was finally adsorbed, as illustrated in Fig. 24. This method leverages the strong covalent bonds between Au-NPs and the SAM, creating a stable and effective platform for protein immobilization. The integration of Au-NPs into SPR biosensors significantly enhances their performance. Starting with a gold substrate, a self-assembled monolayer (SAM) of 1,10-decanedithiol (1,10-DDT) is developed to enable the chemisorption of Au-NPs. The protein is then absorbed onto the Au-NPs, as shown in Fig. 24. Au-NPs increase the local refractive index changes upon biomolecular binding, thereby improving the sensitivity of the SPR signal. This enhancement allows for the detection of lower concentrations of analytes, making Au-NP-modified SPR biosensors particularly useful for applications requiring high sensitivity. The use of SAMs in conjunction with AuNPs provides a versatile and robust approach for the development of SPR biosensors. This combination allows for precise control over the surface chemistry and the spatial arrangement of capture molecules, leading to improved biosensor performance. The ability to tailor the surface properties of the biosensor through SAMs and Au-NPs makes this approach adaptable to a wide range of applications. In conclusion, the integration of gold nanoparticle monolayers into SPR biosensors represents a significant advancement in biosensor technology. The unique properties of Au-NPs, combined with the versatility of SAMs, enable the development of highly

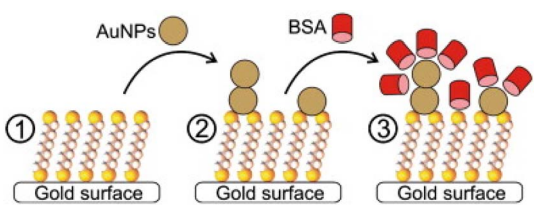

Fig. 24 Fabrication process of the SPR biosensor: formation of 1,10-DDT SAM on gold, chemisorption of Au-NP to 1,10-DDT SAM, immobilization of BSA on AuNP. Reproduced from ref. 73 with permission from [Elsevier], copyright [2009].

sensitive, specific, and reliable biosensors. This technology holds great promise for enhancing the capabilities of SPR biosensors.

6.4.8. Optical biosensors. The development of optical biosensors has seen remarkable progress due to their wide-ranging applications in detecting various biological molecules such as glucose, DNA, *Escherichia coli*, and proteins. These biosensors offer high sensitivity, accuracy, and rapid response, making them invaluable tools in medical diagnostics, environmental monitoring, and food safety. Noble metal nanoparticles, particularly gold (Au), have garnered significant attention in the field of optical biosensors because of their unique, size-dependent optical properties. These nanoparticles exhibit a strong UV-vis absorption band that is absent in the bulk metal. This absorption band appears when the incident photon frequency resonates with the collective excitation of conduction electrons. The UV-vis spectrum of nanoparticles correlates with their size, shape, interparticle spacing, and the dielectric properties of their local environment, including the substrate, solvent, and adsorbates. Au-NPs are especially notable for their ability to form SAMs on various substrates. This capability is exploited in biosensor design to create stable and functional interfaces for biomolecule immobilization. The work of Katherine C. Grabar *et al.*[72] demonstrated that gold colloids could be self-assembled onto a functionalized glass surface, resulting in an optically transparent monolayer stabilized by strong colloid-surface electrostatic interactions. Further studies showed that these immobilized gold colloid monolayers are sensitive to changes in the refractive index of the surrounding solvent and can be used to detect biomolecular interactions. For instance, Okamoto *et al.*[74] demonstrated that the absorbance of an immobilized monolayer of gold colloids is sensitive to the refractive index of the surrounding solvent. Nath and Chilkoti later used an immobilized colloidal Au monolayer to investigate biotin–streptavidin interactions. Kitano's group prepared gold biosensors modified with a self-assembled monolayer of a glucose-carrying polymer chain for the detection of Concanavalin A (Con A), demonstrating real-time biomolecular interaction detection.

Caixin Guo *et al.*[75] reported an improved method for detecting Concanavalin A (Con A) using label-free optical biosensors. In their approach, 1-dodecanethiol (DDT) was self-assembled onto gold nanoparticles deposited on glass slides, followed by the insertion of glycolipid molecules into the DDT layer through physical interactions. The recognition between Con A and the carbohydrate was observed using UV-vis spectrophotometry. When Con A bound to the sugar residues of the glycolipids immobilized on the nanogold slides, a shift in the absorption spectrum was detected, whereas no spectrum change was observed with nonspecific proteins. This self-assembled bilayer structure on nanogold substrates exhibited very high sensitivity for Con A, with a minimum detection concentration of 0.1 nM. Fig. 25 illustrates a schematic depiction of the self-assembled multilayer system used to study biomolecular binding. The simplicity and sensitivity of this biosensor architecture highlights the potential of nanogold applications in biosensors. The self-assembled bilayer structure

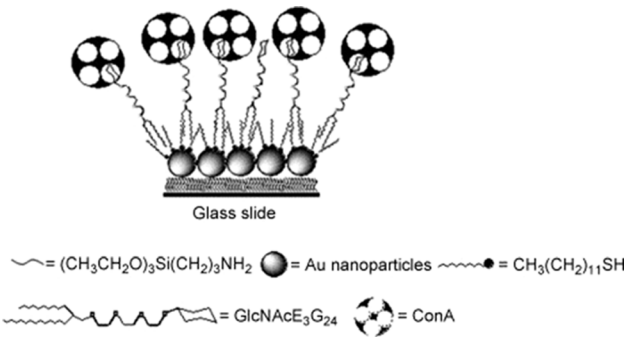

Fig. 25 Diagrammatic representation of the self-assembled multilayer system used for studying biomolecular binding. Reproduced from ref. 72 with permission from [ACS Publications], copyright [1995].

not only offers ultra-sensitivity for investigating carbohydrate–lectin interactions but also simplifies the biosensor fabrication process, eliminating the need for time-consuming organic syntheses required for other receptor immobilizations.[76–82] In summary, gold nanoparticle monolayers play a crucial role in enhancing the performance of optical biosensors. Their unique optical properties, coupled with the ability to form stable and functional self-assembled monolayers, make them ideal for various biosensing applications.[83–94] The integration of Au-NPs into biosensor designs has led to significant advancements in sensitivity, specificity, and simplicity, paving the way for innovative applications in medical diagnostics, environmental monitoring, and beyond.[95–102] The continuous development and refinement of these nanomaterial-based biosensors holds great promise for the future of biosensing technology.[103–112]

Michael Himmelhaus and Hiroyuki Takei[113] presented a novel approach where cap-shaped gold nanoparticles were generated by evaporating gold onto a dense monolayer of randomly adsorbed monodisperse polystyrene (PS) spheres with a diameter of 110 nm. The resulting sample displayed a substantial extinction coefficient of optical density, measuring 2.4 with a bandwidth of 100 nm in the visible region. Interestingly, the position of the extinction peak was found to have a linear dependency on the refractive index of the surrounding environment. This innovative device demonstrated remarkable sensitivity at the sub-monolayer level, as evidenced by its successful detection of octadecanethiolate monolayer formation and biotin/avidin binding. These findings hold significant promise for the development of cost-effective optical biosensors capable of mass parallel detection. Such biosensors have the potential to revolutionize various fields by offering highly sensitive and inexpensive detection methods on a large scale.[114–127]

7. Current challenges

The current challenges in the synthesis, properties, and applications of 2D monolayers of Au-NPs represent a dynamic and rapidly evolving frontier in nanomaterials research. Despite the substantial advancements achieved in recent years, several persistent challenges continue to hinder the widespread

utilization of these materials across various fields. One of the primary challenges lies in the development of efficient, scalable, and environmentally friendly synthesis techniques. Current synthesis routes for Au-NP monolayers often involve complex procedures or require harsh conditions, limiting their applicability and scalability. Additionally, controlling the size and stability of Au-NPs is crucial for their practical utilization. Achieving uniformity in nanoparticle size and ensuring their stability over time presents significant difficulties, as controlling factors such as nucleation, growth, and aggregation during synthesis processes requires further optimization. Surface functionalization of Au-NPs is another critical area that presents challenges. Tailoring the surface chemistry of Au-NPs to impart specific properties and functionalities is essential for their application in diverse fields. However, achieving stable and uniform functionalization while preserving nanoparticle integrity, particularly in complex environments, remains a formidable task. Furthermore, the development of advanced characterization techniques capable of accurately probing the structural, morphological, and chemical properties of Au-NP monolayers at the nanoscale is a pressing need. Current characterization methods often face limitations in terms of resolution, sensitivity, or specificity, making it difficult to fully understand and exploit the properties of these materials.

Integrating Au-NP monolayers into practical devices and systems while maintaining their functionality and stability poses additional challenges. This requires careful consideration of interface engineering, compatibility with other materials, and ensuring long-term performance under operating conditions. Understanding the interfacial phenomena between Au-NP monolayers and their surroundings, including interactions with solvents, substrates, and biomolecules, is crucial for optimizing their performance in diverse applications. However, elucidating these complex interfacial phenomena remains a significant challenge. Scalability and reproducibility are also major concerns. Developing scalable synthesis methods that can produce Au-NP monolayers with reproducible properties is essential for large-scale applications. Unfortunately, many existing techniques are limited in terms of batch-to-batch reproducibility and scalability, which hampers their adoption in industrial processes. Additionally, ensuring the long-term chemical and physical stability of Au-NP monolayers is vital for their practical applications, especially in harsh environments or biological systems. Challenges such as nanoparticle aggregation, oxidation, and degradation over time pose significant hurdles to maintaining the stability of these materials. The tunability of surface plasmon resonance (SPR) properties is another critical challenge. Harnessing the unique optical properties of Au-NPs, such as SPR, for various applications requires precise control over nanoparticle size, shape, and interparticle spacing. Achieving tunable SPR properties while maintaining monolayer integrity is a complex task that necessitates further research and innovation. Moreover, exploiting Au-NP monolayers for biomedical applications requires a thorough assessment of their biocompatibility and potential toxicity. Understanding their interactions with biological systems, minimizing nonspecific binding, and ensuring minimal cytotoxicity and immunogenicity are all critical considerations.

The design of Au-NP monolayers with multifunctional capabilities, such as simultaneous imaging, sensing, and therapeutic functionalities, presents additional challenges. Integrating diverse functionalities while preserving monolayer stability and specificity requires innovative design strategies. Moreover, addressing the environmental impact of Au-NP synthesis and disposal is crucial for sustainable nanotechnology. Developing green synthesis approaches, minimizing waste generation, and enhancing recyclability are essential considerations for mitigating the environmental concerns associated with these materials. Finally, the establishment of standardized protocols for Au-NP monolayer synthesis, characterization, and application is necessary for ensuring consistency, comparability, and safety across different research studies and industrial processes. The development of regulatory frameworks that keep pace with the advancements in this field is also essential to address safety and ethical considerations. Furthermore, enhancing the cost-effectiveness and accessibility of Au-NP monolayers is vital for their widespread adoption across diverse sectors. Reducing production costs, improving material efficiency, and streamlining fabrication processes are necessary steps to democratize the use of these materials. Addressing these challenges will require interdisciplinary efforts spanning chemistry, materials science, physics, and engineering. By overcoming these obstacles, the field of Au-NP monolayers can realize its full potential in revolutionizing applications ranging from healthcare and diagnostics to environmental remediation, energy storage, catalysis, sensing, imaging, drug delivery, and energy conversion.

8. Practical challenges and limitations

Au-NPs monolayers encounter several practical challenges and limitations across their diverse applications. In biosensors, stability remains a significant concern as Au-NP monolayers can degrade over time and under varying environmental conditions like pH and temperature, potentially impacting sensor performance and reliability. Achieving consistent monolayer formation is often challenging, leading to variability in sensor responses. Additionally, ensuring selective binding of target molecules while minimizing non-specific interactions requires precise control, and integrating Au-NP monolayers into practical biosensor devices necessitates compatibility with other materials and processes. For electrochemical applications, uniform monolayer formation on electrode surfaces is critical but challenging due to variations in particle size and shape. These variations can affect the electrical conductivity of the Au-NP monolayers, influencing the efficiency of electrochemical reactions. The long-term stability of these monolayers under operational conditions, such as cycling and potential fluctuations, is also a concern, as it affects the overall durability and performance of electrochemical devices. In electrocatalysis, the catalytic activity of Au-NP monolayers can be constrained by factors such as particle size, shape, and coverage. These factors can impact the effectiveness of catalytic processes. Scaling up

the synthesis of Au-NP monolayers and ensuring their consistent performance for large-scale electrocatalytic applications presents additional challenges. Furthermore, the durability of Au-NP monolayers under harsh operating conditions, such as high currents and aggressive chemical environments, is critical for sustained catalytic activity. For memory systems, integrating Au-NP monolayers requires precise control over nanoparticle placement and alignment, which can be technically demanding. Stability over the operational lifetime of memory devices is essential for reliable performance, and achieving large-area, uniform monolayers involve addressing issues related to consistency and cost. Additionally, the integration process must ensure that the Au-NP monolayers function effectively within the complex architectures of memory devices. Overall, challenges such as the high cost of synthesis, fabrication complexity, and the environmental impact of gold mining and nanoparticle disposal need to be addressed. High-quality synthesis and deposition methods must be optimized, and strategies for enhancing stability and reproducibility must be developed. Additionally, ensuring compatibility with practical device requirements and considering environmental sustainability are crucial for advancing the application of Au-NP monolayers in various technologies.

9. Future prospects

The future prospects of Au-NP monolayer synthesis, properties, and applications are promising, given the rapid advancements in nanotechnology and materials science. Continued research and innovation are expected to address current challenges and unlock new opportunities across various fields. Future developments in Au-NP monolayer synthesis will likely focus on more precise, scalable, and cost-effective methods. Techniques such as microcontact printing, laser ablation, and chemical vapor deposition (CVD) may be further refined to produce uniform and stable monolayers. The use of greener synthesis approaches, minimizing the use of harmful solvents and reducing waste, will also become increasingly important. Advancements in understanding the fundamental properties of Au-NP monolayers will enable the design of materials with highly specific and tunable properties. Researchers are expected to develop methods to the ordered structure of Au NPs in the monolayer film (reducing the defects in the Au NPs in the monolayer film). This will be crucial for applications in sensors, catalysis, and electronics. The use of ligand exchange reactions to modify the surface chemistry of Au-NPs can lead to tailored functionalities and improved performance in specific applications. Improving the long-term stability and durability of Au-NP monolayers will be a key focus area. Innovations in surface modification techniques, such as the use of protective coatings and stabilizing ligands, will help prevent nanoparticle aggregation and oxidation. This will be particularly important for applications in harsh environments and in biomedical devices. The biocompatibility and unique optical properties of Au-NP monolayers make them ideal candidates for biomedical applications. Future research will likely explore their use in targeted drug delivery, imaging, and diagnostic applications.

Functionalizing Au-NPs with specific biomolecules will enable highly selective interactions with biological targets, enhancing the efficacy and safety of therapeutic interventions. Au-NP monolayers hold significant potential for environmental remediation and energy-related applications. Future research may focus on developing highly efficient catalysts for water purification, carbon capture, and renewable energy conversion processes. The integration of Au-NP monolayers into solar cells and fuel cells could lead to significant improvements in their performance and efficiency. The development of multifunctional devices incorporating Au-NP monolayers will be a major area of growth. These devices could combine sensing, imaging, and therapeutic functions into a single platform, enabling new approaches to disease diagnosis and treatment. The versatility of Au-NPs will also allow for their integration into flexible and wearable electronics, opening up new possibilities for personalized healthcare. As the use of Au-NP monolayers expands, establishing standardized protocols for their synthesis, characterization, and application will be essential. Regulatory frameworks will need to evolve to address safety, ethical, and environmental considerations associated with the production and use of nanomaterials. Ensuring consistency and safety will be critical for gaining public trust and facilitating widespread adoption. Theoretical and computational studies will play a vital role in guiding experimental efforts and understanding the behavior of Au-NP monolayers at the atomic level. Density functional theory (DFT) and molecular dynamics simulations can provide insights into the electronic structure, stability, and reactivity of Au-NPs, helping to predict and optimize their properties for various applications. In summary, the future of Au-NP monolayers is bright, with numerous opportunities for innovation and application across diverse fields. Continued research and collaboration among scientists, engineers, and policymakers will be crucial for overcoming current challenges and realizing the full potential of these versatile nanomaterials.

10. Conclusions

In summary, the field of 2D Au-NP monolayers presents a vibrant and rapidly evolving landscape, driven by a profound understanding of the underlying chemistry and the interplay of various interactions. Electrostatic forces, van der Waals attractions, and ligand-mediated stabilization are pivotal in directing the self-assembly of Au-NPs into robust and functional monolayers. The size and shape of nanoparticles play crucial roles in determining the structural and functional properties of these monolayers, influencing their formation and stability across different interfaces. The diverse applications of Au-NP monolayers in memory devices, biosensors, and electrocatalysis underscore their versatility and potential to revolutionize these fields. Their exceptional electron transport properties, sensitivity, and catalytic efficiency make them indispensable in advancing technology. However, challenges such as scalability, reproducibility, and long-term stability remain significant obstacles that need to be addressed. Future research should focus on developing innovative strategies to overcome these challenges, such as enhancing the synthesis and assembly

processes, improving material stability, and exploring new functionalizations. Additionally, integrating Au-NP monolayers with other nanomaterials could unlock new capabilities and applications, further broadening their impact. Ultimately, the continued exploration and refinement of 2D Au-NP monolayers will not only deepen our understanding of nanoscale interactions and assembly but also drive the development of next-generation technologies across various sectors. The journey ahead is promising, with the potential to achieve breakthroughs that could transform current technological paradigms.

Abbreviations

Au-NPs	Gold nanoparticles
Au-ene	Goldene
SPR	Surface plasmon resonance
2D	Two-dimensional
AFM	Atomic force microscopy
STM	Scanning tunneling microscopy
DLVO	Derjaguin–Landau–Verwey–Overbeek
U	Interaction energy
A	Hamaker constant
Π	Surface pressure
F	Force
A	Area
XPS	X-ray photoelectron spectroscopy
FTIR	Fourier-transform infrared spectroscopy
F_{vdW}	Van der Waals
F_{elec}	Electrostatic
F_{steric}	Steric interactions
C_{eq}	Surface coverage
R	Gas constant
T	Temperature
ΔG	Gibbs free energy
LB	Langmuir–Blodgett method
EPD	Electrophoretic deposition method
PMMA	Poly(methyl methacrylate)
ITO	Indium tin oxide
MSTFs	Mesoporous silica thin films
MSNs	Mesoporous silica nanoparticles
SERS	Surface-enhanced Raman spectroscopy
RFID	Radio frequency identification
MOS	Metal-oxide-semiconductor
Al_2O_3	Aluminum oxide
C-AFM	Conductive mode atomic force microscopy
PET	Polyethylene terephthalate
TEM	Transmission electron microscopy
SONOS	Silicon–oxide–nitride–oxide–silicon devices
NC	Nanocrystal
BOD	Bilirubin oxidases
LAC	Laccase
SAMs	Self-assembled monolayers
ITO	Indium tin oxide
CVs	Cyclic voltammograms
Mv BOD	*Myrothecium verrucaria* bilirubin oxidase
BDD	Boron-doped diamond substrates
DTSP	Dithiobis-*N*-succinimidyl propionate
TDT	Inert tetradecane-1-thiol
MPA	3-Mercaptopropionic acid
AchE	Amperometric acetylcholinesterase
GO_x	Glucose oxidase
CVD	Chemical vapor deposition

Data availability

The data supporting this study's findings are available from the corresponding author upon reasonable request.

Conflicts of interest

There are no conflicts to declare.

Acknowledgements

This work was supported by Khalifa University of Science and Technology, under funding grant number RIG-2023-027.

References

1 E. C. Dreaden, A. M. Alkilany, X. Huang, C. J. Murphy and M. A. El-Sayed, *Chem. Soc. Rev.*, 2012, **41**, 2740–2779.
2 Y. A. Almehmadi, J. McGeehan, N. J. Guzman, K. E. Christensen, K. Yamazaki and D. J. Dixon, Iridium-catalysed synthesis of *C,N,N*-cyclic azomethine imines enables entry to unexplored nitrogen-rich 3D chemical space, *Nat. Synth.*, 2024, **3**, 1168–1175, DOI: **10.1038/s44160-024-00574-w**.
3 S. Soodi, J. J. Zhang, J. Zhang, Y. Liu, M. Lashgari, S. Zafeiratos, A. Züttel, K. Zhao and W. Luo, Selective electroreduction of CO_2 to C_{2+} products on cobalt decorated copper catalysts, *Chem. Synth.*, 2024, **4**, 44, DOI: **10.20517/cs.2024.11**.
4 C. Song, L. Xiao, Y. Chen, F. Yang, H. Meng, W. Zhang, Y. Zhang and Y. Wu, "TiO_2-Based Catalysts with Various Structures for Photocatalytic Application: A Review", *Catalysts*, 2024, **14**(6), 366, DOI: **10.3390/catal14060366**.
5 C. Burns, W. U. Spendel, S. Puckett and G. E. Pacey, Solution ionic strength effect on gold nanoparticle solution color transition, *Talanta*, 2006, **69**(4), 873–876, DOI: **10.1016/j.talanta.2005.11.038**.
6 A. B. Smith, C. D. Jones and E. Johnson, Electrostatic assembly of two-dimensional gold nanoparticle monolayers on positively charged surfaces, *Langmuir*, 2018, **34**(20), 5796–5803.
7 X. Chen, L. Wang and H. Zhang, Controllable assembly of two-dimensional gold nanoparticle monolayers on negatively charged substrates via electrostatic interactions, *J. Colloid Interface Sci.*, 2021, **585**, 110–117.
8 J. Wang, L. Zhang and Y. Liu, Tuning the assembly of gold nanoparticles on substrates via van der Waals interactions, *Langmuir*, 2019, **35**(9), 3326–3333.
9 X. Li, C. Wang and H. Zhang, Comparative study of assembly kinetics of gold nanoparticles driven by van der

Waals forces and electrostatic interactions, *J. Colloid Interface Sci.*, 2020, **579**, 691–698.
10 Y. Liu, T. Li and L. Zhang, Highly ordered two-dimensional arrays of gold nanoparticles with controlled interparticle spacing for surface-enhanced Raman scattering, *ACS Appl. Mater. Interfaces*, 2017, **9**(23), 19928–19934.
11 Q. Zhang, J. Wang and B. Liu, Tuning the plasmonic properties of two-dimensional gold nanoparticle monolayers through ligand engineering, *Langmuir*, 2019, **35**(6), 2306–2313.
12 F. Zhang, S. Wu and Y. Lu, Synthesis of Gold Nanoparticles for in Vitro Diagnostics, in *Advanced Concepts in Fluorescence Sensing*, Springer, Berlin, Heidelberg, 2012, pp. 201–224.
13 Z. Nie, A. Petukhova and E. Kumacheva, Properties and emerging applications of self-assembled structures made from inorganic nanoparticles, *Nat. Nanotechnol.*, 2017, **5**(1), 15–25.
14 Y. Liu, H. Zhang and H. Yang, Surface chemistry and ligand-mediated self-assembly of nanoparticles, *Chem. Soc. Rev.*, 2019, **48**(6), 1629–1656.
15 A. B. Smith, C. D. Jones and E. F. Johnson, Shape-dependent self-assembly of gold nanoparticles, *J. Mater. Chem. A*, 2015, **3**(25), 13216–13222.
16 L. Wang, H. Zhang and X. Chen, Solvent effects on the self-assembly behavior of gold nanoparticles with various shapes, *Langmuir*, 2020, **36**(15), 4145–4153.
17 C. Huang, J. Sun, Z. Xue, X. Cai and H. Li, Ligand Length Modulates the Self-Assembly of Gold Nanoparticles at the Water-Air Interface, *Langmuir*, 2015, **31**(4), 1375–1381, DOI: **10.1021/la5042082**.
18 A. M. Smith, S. Nie and Y. Nakamura, Dynamics of Gold Nanoparticles at the Aqueous Solution/Air Interface Revealed by Time-Resolved X-ray Reflectivity, *J. Phys. Chem. Lett.*, 2018, **9**(20), 6060–6066, DOI: **10.1021/acs.jpclett.8b02404**.
19 J. Lee, J. Kang and S. G. Im, Self-Assembly of Gold Nanoparticles on Substrates via Solvent Evaporation: The Effects of Nanoparticle Size, Surface Chemistry, and Substrate Wettability, *Langmuir*, 2016, **32**(6), 1523–1531, DOI: **10.1021/acs.langmuir.5b03821**.
20 Y. Zhang, Y. Cao, X. Jiang and Z. Yu, Controlled Self-Assembly of Gold Nanoparticles on a Solid Substrate: From Disorder to Order, *Langmuir*, 2019, **35**(22), 7103–7109, DOI: **10.1021/acs.langmuir.9b00353**.
21 J. Wang, D. Wang, N. S. Sobal, M. Giersig, M. Jiang and H. Möohwald, *Angew. Chem., Int. Ed.*, 2006, 7963–7966.
22 J.-W. Hu, G.-B. Han, B. Ren, S. Shi-Gang and Z.-Q. Tian, *Langmuir*, 2004, **20**, 8831–8838.
23 F. Reincke, W. K. Kegel, H. Zhang, M. Nolte, D. Wang, D. Vanmaekelbergh and H. Möhwald, *Phys. Chem. Chem. Phys.*, 2006, **8**, 3828–3835.
24 K. Y. Lee, M. Kim, J. Hahn, J. S. Suh, I. Lee, K. Kim and S. W. Han, *Langmuir*, 2006, **22**, 1817–1821.
25 H. Duan, D. Wang, D. G. Kurth and H. Möhwald, *Angew. Chem., Int. Ed.*, 2004, 5639–5642.
26 F. Reincke, S. G. Hickey, W. K. Kegel and D. Vanmaekelbergh, *Angew. Chem., Int. Ed.*, 2004, 458–462.
27 Y.-J. Li, W.-J. Huang and S.-G. Sun, *Angew. Chem., Int. Ed.*, 2006, 2537–2539.
28 M.-H. Wang, J.-W. Hu, Y.-J. Li1 and E. S. Yeung, Au nanoparticle monolayers: preparation, structural conversion and their surface-enhanced Raman scattering effects, *Nanotechnology*, 2010, **21**, 145608, DOI: **10.1088/0957-4484/21/14/145608**.
29 T. Ming, X. Kou, H. Chen, T. Wang, H. L. Tam, K. W. Cheah, J. Y. Chen and J. Wang, *Angew. Chem., Int. Ed.*, 2008, **47**, 9685–9690.
30 C.-M. H. Shen and T.-S. Wong, *J. Phys. Chem. B*, 2010, **114**, 5269–5274.
31 F. Ahmad Deader, Y. Abbas, A. Qurashi, M. Al-Qutayri, V. Chan and M. Rezeq, Electric Field-Driven Self-Assembly of Gold Nanoparticle Monolayers on Silicon Substrates, *Langmuir*, 2023, **39**(44), 15766–15772, DOI: **10.1021/acs.langmuir.3c02351**.
32 S. Kashiwaya, Y. Shi, J. Lu, D. G. Sangiovanni, G. Greczynski, M. Magnuson, M. Andersson, J. Rosen and L. Hultman, Synthesis of goldene comprising single-atom layer gold, *Nat. Synth.*, 2024, **3**, 744–751, DOI: **10.1038/s44160-024-00518-4**.
33 P. Sarkar and P. S. Nicholson, Electrophoretic Deposition (EPD): Mechanisms, Kinetics, and Application to Ceramics, *J. Am. Ceram. Soc.*, 1996, **79**, 1987–2002.
34 K. W. Song, R. Costi and V. Bulović, Electrophoretic Deposition of CdSe/Zns Quantum Dots for Light-Emitting Devices, *Adv. Mater.*, 2013, **25**, 1420–1423.
35 P. Sarkar, X. Haung and P. S. Nicholson, Structural Ceramic Micro laminates by Electrophoretic Deposition, *J. Am. Ceram. Soc.*, 1992, **75**, 2907–2909.
36 M. Giersig and P. Mulvaney, Preparation of Ordered Colloid Monolayers by Electrophoretic Deposition, *Langmuir*, 1993, **9**, 3408–3413.
37 P. Brown and P. V. Kamat, Quantum Dot Solar Cells. Electrophoretic Deposition of CdSe−C60 Composite Films and Capture of Photogenerated Electrons with nC60 Cluster Shell, *J. Am. Chem. Soc.*, 2008, **130**, 8890–8891.
38 A. A. Shah, M. Ganesan, J. Jocz and M. J. Solomon, Direct Current Electric Field Assembly of Colloidal Crystals Displaying Reversible Structural Color, *ACS Nano*, 2014, **8**, 8095–8103.
39 A. A. Shah, H. Kang, K. L. Kohlstedt, K. H. Ahn, S. C. Glotzer, C. W. Monroe and M. J. Solomon, Liquid Crystal Order in Colloidal Suspensions of Spheroidal Particles by Direct Current Electric FieldAssembly, *Small*, 2012, **8**, 1551–1562.
40 D. Prieve, J. Anderson, J. Ebel and M. Lowell, Motion of a Particle Generated by Chemical Gradients. Part 2. Electrolytes, *J. Fluid Mech.*, 1984, **148**, 247–269.
41 D. C. Prieve, P. J. Sides and C. L. Wirth, 2-D Assembly ofColloidal Particles on a Planar Electrode, *Curr. Opin. Colloid Interface Sci.*, 2010, **15**, 160–174.
42 K. D. Barbee, A. P. Hsiao, M. J. Heller and X. Huang, Electric Field Directed Assembly of High-Density Microbead Arrays, *Lab Chip*, 2009, **9**, 3268–3274.

43 F. Qian, A. J. Pascall, M. Bora, T. Y.-J. Han, S. Guo, S. S. Ly, M. A. Worsley, J. D. Kuntz and T. Y. Olson, On-Demand and Location Selective Particle Assembly Via Electrophoretic Deposition for Fabricating Structures with Particle-to-Particle Precision, *Langmuir*, 2015, **31**, 3563–3568.

44 H. Zhang, J. Cadusch, C. Kinnear, T. James, A. Roberts and P. Mulvaney, *ACS Nano*, 2018, **12**, 7529–7537.

45 X. Xiong, P. Makaram, A. Busnaina, K. Bakhtari, S. Somu, N. McGruer and J. Park, Large Scale Directed Assembly of Nanoparticles Using Nanotrench Templates, *Appl. Phys. Lett.*, 2006, **89**, 193108.

46 Yi-W. Wang, K.-C. Kao, J.-K. Wang and C.-Y. Mou, Large-Scale Uniform Two-Dimensional Hexagonal Arrays of Gold Nanoparticles Templated from Mesoporous Silica Film for Surface-Enhanced Raman Spectroscopy, *J. Phys. Chem. C*, 2016, **120**(42), 24382–24388, DOI: **10.1021/acs.jpcc.6b08116**.

47 A. Rezk, Y. Abbas, I. Saadat, A. Nayfeh and M. Rezeq, Charging and discharging characteristics of a single gold nanoparticle embedded in Al_2O_3 thin films, *Appl. Phys. Lett.*, 2020, **116**, 223501, DOI: **10.1063/5.0004000**.

48 Y. Abbas, A. Rezk, I. Saadat, A. Nayfeh and M. Rezeq, Time dependence of electrical characteristics during the charge decay from a single gold nanoparticle on silicon, *RSC Adv.*, 2020, **10**, 41741–41746, DOI: **10.1039/D0RA08135C**.

49 Ye Zhou, Su-T. Han, Z.-X. Xu and V. A. L. Roy, The strain and thermal induced tunable charging phenomenon in low power flexible memory arrays with a gold nanoparticle monolayer, *Nanoscale*, 2013, **5**, 1972, DOI: **10.1039/c2nr32579a**.

50 S.-T. Han, Y. Zhou, Z.-X. Xu, L.-B. Huang, X.-B. Yang and V. A. L. Roy, Microcontact Printing of Ultrahigh Density Gold Nanoparticle Monolayer for Flexible Flash Memories, *Adv. Mater.*, 2012, **24**, 3556–3561, DOI: **10.1002/adma.201201195**.

51 S. J. Kim, Y. S. Park, S. H. Lyu and J. S. Lee, *Appl. Phys. Lett.*, 2010, **96**, 033302.

52 H. Abunahla, Y. Abbas, A. Gebregiorgis, W. Waheed, M. Baker, S. Hamdioui, A. Alazzam and M. Rezeq, Analog monolayer SWCNTs-based memristive 2D structure for energy-efficient deep learning in spiking neural networks, *Sci. Rep.*, 2023, **13**, 21350, DOI: **10.1038/s41598-023-48529-z**.

53 M. Umair Khan, Y. Abbas, H. Abunahla, M. Rezeq, A. Alazzam, N. Alamoodi and M. Baker, Biocompatible humidity sensor using paper cellulose fiber/GO matrix for human health and environment monitoring, *Sens. Actuators, B*, 2023, **393**, 134188.

54 S. Anwer, M. U. Khan, M. Baker, M. Rezeq, W. Cantwell, D. Gan and L. Zheng, Engineering of electrodes with 2D $Ti_3C_2T_x$-MXene sheets and chloride salt for robust and flexible high electrical power triboelectric nanogenerator, *Chem. Eng. J.*, 2023, **470**, 144281.

55 D. Ji, X. Li, M. Rezeq, W. Cantwell and L. Zheng, Long-Term Stable Thermal Emission Modulator Based on Single-Walled Carbon Nanotubes, *ACS Appl. Mater. Interfaces*, 2023, **15**(31), 37818–37827, DOI: **10.1021/acsami.3c06952**.

56 L. Tizani, Y. Abbas, M. Y. Ahmed, M. Baker and M. Rezeq, Single wall carbon nanotube based optical rectenna, *RSC Adv.*, 2021, **11**, 24116–24124, DOI: **10.1039/D1RA04186J**.

57 Y. Abbas, M. Rezeq, A. Nayfeh and I. Saadat, Size dependence of charge retention in gold-nanoparticles sandwiched between thin layers of titanium oxide and silicon oxide, *Appl. Phys. Lett.*, 2021, **119**, 162103, DOI: **10.1063/5.0063515**.

58 M. Umair Khan, E. Mohammad, Y. Abbas, M. Rezeq and M. Baker, Chicken skin based Milli Watt range biocompatible triboelectric nanogenerator for biomechanical energy harvesting, *Sci. Rep.*, 2023, **13**, 10160.

59 T. McArdle, T. P. McNamara, F. Fei and C. F. Blanford, Optimizing the mass-specific activity of bilirubin oxidase adlayers through combined electrochemical quartz crystal microbalance and dual polarization interferometry analyses, *ACS Appl. Mater. Interfaces*, 2015, **7**, 25270–25280, DOI: **10.1021/acsami.5b07290**.

60 V. P. Hitaishi, I. Mazurenko, A. Vengasseril Murali, A. de Poulpiquet, G. Coustillier, P. Delaporte and E. Lojou, Nanosecond Laser–Fabricated Monolayer of Gold Nanoparticles on ITO for Bioelectrocatalysis, *Front. Chem.*, 2020, **8**, 431, DOI: **10.3389/fchem.2020.00431**.

61 Ru-hai Tian, T. N. Rao, Y. Einaga and Z. Jin-fang, Construction of Two-Dimensional Arrays Gold Nanoparticles Monolayer onto Boron-Doped Diamond Electrode Surfaces, *Chem. Mater.*, 2006, **18**, 939–945, DOI: **10.1021/cm0519481**.

62 N. Zhou, J. Wang, T. Chen, Z. Yu and G. Li, Enlargement of Gold Nanoparticles on the Surface of a Self-Assembled Monolayer Modified Electrode: A Mode in Biosensor Design, *Anal. Chem.*, 2006, **78**, 5227–5230, DOI: **10.1021/ac0605492**.

63 B.-W. Park, D.-S. Kim and Do-Y. Yoon, Surface modification of gold electrode with gold nanoparticles and mixed self-assembled monolayers for enzyme biosensors, *Korean J. Chem. Eng.*, 2011, **28**(1), 64–70, DOI: **10.1007/s11814-010-0349-6**.

64 M. Çetin Canbaz, Ç. Sayıklı Şimşek and M. Kemal Sezgintürk, Electrochemical biosensor based on self-assembled monolayers modified with gold nanoparticles for detection of HER-3, *Anal. Chim. Acta*, 2014, **814**, 31–38, DOI: **10.1016/j.aca.2014.01.041**.

65 M. Ratna Kumalasari, R. Alfanaar and A. Sus Andreani, Gold nanoparticles (AuNPs): A versatile material for biosensor application, *Talanta*, 2024, **9**, 100327.

66 D. Du, J. Ding, J. Cai, J. Zhang and L. Liu, In situ electrodeposited nanoparticles for facilitating electron transfer across self-assembled monolayers in biosensor design, *Talanta*, 2008, **74**(5), 1337–1343, DOI: **10.1016/j.talanta.2007.09.003**.

67 M. L. Mena, P. Yáñez-Sedeño and J. M. Pingarrón, A comparison of different strategies for the construction of amperometric enzyme biosensors using gold nanoparticle-modified electrodes, *Anal. Biochem.*, 2005, **336**(1), 20–27, DOI: **10.1016/j.ab.2004.07.038**.

68 F. Arduini, S. Guidone, A. Amine, G. Palleschi and D. Moscone, Acetylcholinesterase biosensor based on self-assembled monolayer-modified gold-screen printed electrodes for organophosphorus insecticide detection, *Sens. Actuators, B*, 2013, **179**, 201–208, DOI: 10.1016/j.snb.2012.10.016.
69 F. Li, Y. Feng, P. Dong and B. Tang, Gold nanoparticles modified electrode via a mercapto-diazoaminobenzene monolayer and its development in DNA electrochemical biosensor, *Biosens. Bioelectron.*, 2010, **25**(9), 2084–2088, DOI: 10.1016/j.bios.2010.02.004.
70 S. Balamurugan, A. Obubuafo, S. A. Soper, R. L. McCarley and D. A. Spivak, Designing Highly Specific Biosensing Surfaces Using Aptamer Monolayers on Gold, *Langmuir*, 2006, **22**(14), 6446–6453, DOI: 10.1021/la060222w.
71 X. Zhong, R. Yuan, Y. Chai, Y. Liu, J. Dai and D. Tang, Glucose biosensor based on self-assembled gold nanoparticles and double-layer 2d-network (3-mercaptopropyl)-trimethoxysilane polymer onto gold substrate, *Sens. Actuators, B*, 2005, **104**(2), 191–198, DOI: 10.1016/j.snb.2004.04.114.
72 K. C. Grabar, R. G. Freeman, M. B. Hommer and M. J. Natan, Preparation and Characterization of Au Colloid Monolayers, *Anal. Chem.*, 1995, **67**(4), 735–743, DOI: 10.1021/ac00100a008.
73 E. M. S. Azzam, A. Bashir, O. Shekhah, A. R. E. Alawady, A. Birkner, Ch. Grunwald and Ch. Wöll, Fabrication of a surface plasmon resonance biosensor based on gold nanoparticles chemisorbed onto a 1,10-decanedithiol self-assembled monolayer, *Thin Solid Films*, 2009, **518**(1), 387–391, DOI: 10.1016/j.tsf.2009.07.120.
74 T. Okamoto, I. Yamaguchi and T. Kobayashi, "Local plasmon sensor with gold colloid monolayers deposited upon glass substrates", *Opt. Lett.*, 2000, **25**, 372–374.
75 C. Guo, P. Boullanger, L. Jiang and T. Liu, Highly sensitive gold nanoparticles biosensor chips modified with a self-assembled bilayer for detection of Con A, *Biosens. Bioelectron.*, 2007, **22**(8), 1830–1834, DOI: 10.1016/j.bios.2006.09.006.
76 M. Rezeq, Y. Abbas, B. Wen, Z. Wasilewski and D. Ban, Physical probing of quantum energy levels in a single indium arsenide (InAs) quantum dot, *Nanoscale Adv.*, 2023, **5**, 5562–5569.
77 Y. Abbas, M. U. Khan, F. Ravaux, M. Baker and M. Rezeq, Focused ion beam engineering of carbon nanotubes for optical rectenna applications, *ACS Appl. Nano Mater.*, 2022, **5**, 18537–18544.
78 S. Anwer, Y. Abbas, F. Ravaux, D. H. Anjum, M. Rezeq, M. Baker, T. D. Dongale, K. Liao, W. Cantwell, D. Gan and L. Zheng, Cobalt oxide nanoparticles embedded in borate matrix: A conduction mode atomic force microscopy approach to induce nano-memristor switching for neuromorphic applications, *Appl. Mater. Today*, 2022, **29**, 101691.
79 S. Shan, W. Zhao, J. Luo, J. Yin, J. C. Switzer, P. Joseph, S. Lu, M. Poliks and C.-J. Zhong, *J. Mater. Chem. C*, 2014, **2**, 1893.
80 Rezeq, Y. Abbas, B. Wen, Z. Wasilewski and D. Ban, Direct detection of electronic states for individual indium arsenide (InAs) quantum dots grown by molecular beam epitaxy, *Appl. Surf. Sci.*, 2022, **590**, 153046.
81 M. 'd Rezeq, Nanotips with a single atom end as ideal sources of electron and ion beams: Modeling of the nanotip shape, *Microelectron. Eng.*, 2013, **102**, 2–5, DOI: 10.1016/j.mee.2012.02.014.
82 M. 'd Rezeq, Finite element simulation and analytical analysis for nano field emission sources that terminate with a single atom: A new perspective on nanotips, *Appl. Surf. Sci.*, 2011, **258**(5), 1750–1755, DOI: 10.1016/j.apsusc.2011.10.034.
83 M. 'd Rezeq, C. Joachim and N. Chandrasekhar, Nanotip apex modification with atomic precision and single atom tips restoration, *Microelectron. Eng.*, 2009, **86**(4–6), 996–998, DOI: 10.1016/j.mee.2008.10.022.
84 L. Song, Y. Huang, Z. Nie and T. Chen, Macroscopic two-dimensional monolayer films of gold nanoparticles: fabrication strategies, surface engineering and functional applications, *Nanoscale*, 2020, **12**, 7433.
85 P. Zijlstra, J. W. M. Chon and M. Gu, *Nature*, 2009, **459**, 410–413.
86 A. S. Roberts, S. M. Novikov, Y. Yang, Y. Chen, S. Boroviks, J. Beermann, N. A. Mortensen and S. I. Bozhevolnyi, *ACS Nano*, 2019, **13**, 71–77.
87 H. Wohltjen and A. W. Snow, *Anal. Chem.*, 1998, **70**, 2856–2859.
88 Z. Nie, D. Fava, M. Rubinstein and E. Kumacheva, *J. Am. Chem. Soc.*, 2008, **130**, 3683–3689.
89 Y. Wang, A. E. DePrince 3rd, S. K. Gray, X. M. Lin and M. Pelton, *J. Phys. Chem. Lett.*, 2010, **1**, 2692–2698.
90 N. Olichwer, A. Meyer, M. Yesilmen and T. Vossmeyer, *J. Mater. Chem. C*, 2016, **4**, 8214–8225.
91 W. P. Wuelfing, S. J. Green, J. J. Pietron, D. E. Cliffel and R. W. Murray, *J. Am. Chem. Soc.*, 2000, **122**, 11465–11472.
92 N. Olichwer, E. W. Leib, A. H. Halfar, A. Petrov and T. Vossmeyer, *ACS Appl. Mater. Interfaces*, 2012, **4**, 6151–6161.
93 E. García-Berríos, T. Gao, J. C. Theriot, M. D. Woodka, B. S. Brunschwig and N. S. Lewis, *J. Phys. Chem. C*, 2011, **115**, 6208–6217.
94 R. A. Potyrailo, M. Larsen and O. Riccobono, *Angew. Chem., Int. Ed.*, 2013, **52**, 10360–10364.
95 N. Shehada, J. C. Cancilla, J. S. Torrecilla, E. S. Pariente, G. Bronstrup, S. Christiansen, D. W. Johnson, M. Leja, M. P. Davies, O. Liran, N. Peled and H. Haick, *ACS Nano*, 2016, **10**, 7047–7057.
96 Y. Y. Broza, P. Mochalski, V. Ruzsanyi, A. Amann and H. Haick, *Angew. Chem., Int. Ed.*, 2015, **54**, 11036–11048.
97 V. Ruzsanyi, W. Lederer, C. Seger, B. Calenic, K. R. Liedl and A. Amann, *J. Breath Res.*, 2014, **8**, 046005.
98 M. Segev-Bar and H. Haick, *ACS Nano*, 2013, **7**, 8366–8378.
99 T. P. Huynh and H. Haick, *Adv. Mater.*, 2016, **28**, 138–143.
100 Z. Mei and L. Tang, *Anal. Chem.*, 2017, **89**, 633–639.
101 H. Ko, S. Singamaneni and V. V. Tsukruk, *Small*, 2008, **4**, 1576–1599.

102 B. N. Khlebtsov, V. A. Khanadeev, M. Y. Tsvetkov, V. N. Bagratashvili and N. G. Khlebtsov, *J. Phys. Chem. C*, 2013, **117**, 23162–23171.
103 V. Liberman, C. Yilmaz, T. M. Bloomstein, S. Somu, Y. Echegoyen, A. Busnaina, S. G. Cann, K. E. Krohn, M. F. Marchant and M. Rothschild, *Adv. Mater.*, 2010, **22**, 4298–4302.
104 A. Campion and P. Kambhampati, *Chem. Soc. Rev.*, 1998, **27**, 241.
105 J. F. Betz, W. W. Yu, Y. Cheng, I. M. White and G. W. Rubloff, *Phys. Chem. Chem. Phys.*, 2014, **16**, 2224–2239.
106 S. L. Kleinman, R. R. Frontiera, A. I. Henry, J. A. Dieringer and R. P. Van Duyne, *Phys. Chem. Chem. Phys.*, 2013, **15**, 21–36.
107 X. Y. L. Martin, J. Mulvihill, J. Henzie and P. Yang, *J. Am. Chem. Soc.*, 2010, **132**, 268–274.
108 Q. Li, Y. Jiang, R. Han, X. Zhong, S. Liu, Z. Y. Li, Y. Sha and D. Xu, *Small*, 2013, **9**, 927–932.
109 H. Dai, S. Chen, Y. Li, B. Zeng, S. Zhang, Z. Hong and Y. Lin, *Biosens. Bioelectron.*, 2017, **92**, 687–694.
110 X. Kong, Q. Yu, X. Zhang, X. Du, H. Gong and H. Jiang, *J. Mater. Chem.*, 2012, **22**, 7767.
111 B. Kokuoz, K. G. Kornev and I. Luzinov, *ACS Appl. Mater. Interfaces*, 2009, **1**, 575–583.
112 J. Hrabakova, K. Ataka, J. Heberle, P. Hildebrandt and D. H. Murgida, *Phys. Chem. Chem. Phys.*, 2006, **8**, 759–766.
113 M. Himmelhaus and H. Takei, Cap-shaped gold nanoparticles for an optical biosensor, *Sens. Actuators, B*, 2000, **63**(1–2), 24–30, DOI: **10.1016/S0925-4005(99)00393-7**.
114 J. Kim, M. Lee, C. Song, J.-K. Song, J. Koo, D. Lee, H. Shim, J. Kim, M. Lee, T. Hyeon and D. Kim, *Sci. Adv.*, 2016, **2**, e1501101.
115 Y. Liu, S. Yu, R. Feng, A. Bernard, Y. Liu, Y. Zhang, H. Duan, W. Shang, P. Tao, C. Song and T. Deng, *Adv. Mater.*, 2015, **27**, 2768–2774.
116 K. Bae, G. Kang, S. K. Cho, W. Park, K. Kim and W. J. Padilla, *Nat. Commun.*, 2015, **6**, 10103.
117 K. Zhang, J. Zhao, J. Ji, Y. Li and B. Liu, *Anal. Chem.*, 2015, **87**, 8702–8708.
118 M. Nguyen, N. Felidj and C. Mangeney, *Chem. Mater.*, 2016, **28**, 3564–3577.
119 T. Ramachandran, M. P. Pachamuthu, G. Karthikeyan, F. Hamed and M. Rezeq, Synergistic effects in CuO/SnO_2/$Ti_3C_2T_x$ nanohybrids: Unveiling their potential as supercapacitor cathode material, *Mater. Sci. Semicond. Process.*, 2024, **179**, 108486, DOI: **10.1016/j.mssp.2024.108486**.
120 T. S. Sreeprasad and T. Pradeep, *Langmuir*, 2011, **27**, 3381–3390.
121 A. Lukach, K. Liu, H. Therien-Aubin and E. Kumacheva, *J. Am. Chem. Soc.*, 2012, **134**, 18853–18859.
122 T. Ramachandran, H. Butt, L. Zheng and M. Rezeq, A review of 2D metal boride-derived nanostructures: From synthesis to energy storage and conversion applications, *J. Energy Storage*, 2024, 113425, DOI: **10.1016/j.est.2024.113425**.
123 T. Wang, J. Lynch, O. Chen, Z. Wang, X. Wang, D. LaMontagne, H. Wu, Z. Wang and Y. C. Cao, *Science*, 2012, **338**, 358–363.
124 Y. Anil Kumar, N. Roy, T. Ramachandran, H. Mohamed, Md Moniruzzaman and S. W. Joo, Shaping the future of energy: The rise of supercapacitors progress in the last five years, *J. Energy Storage*, 2024, **98**, 113040, DOI: **10.1016/j.est.2024.113040**.
125 M. Zanella, R. Gomes, M. Povia, C. Giannini, Y. Zhang, A. Riskin, M. Van Bael, Z. Hens and L. Manna, *Adv. Mater.*, 2011, **23**, 2205–2209.
126 K. S. Y. A. Baloushi, A. Senthilkumar, K. Kandhan, R. Subramanian, J. Kizhakkayil, T. Ramachandran, S. Shehab, S. S. Kurup, M. A. M. Alyafei, A. S. A. Dhaheri and A. Jaleel, Green Synthesis and Characterization of Silver Nanoparticles Using Moringa Peregrina and Their Toxicity on MCF-7 and Caco-2 Human Cancer Cells, *Int. J. Nanomed.*, 2024, **19**, 3891–3905, DOI: **10.2147/IJN.S451694**.
127 Y. Anil Kumar, J. Kumar Alagarasan, T. Ramachandran, M. Rezeq, M. A. Bajaber, A. A. Alalwiat, Md Moniruzzaman and M. Lee, The landscape of energy storage: Insights into carbon electrode materials and future directions, *J. Energy Storage*, 2024, **86**, 111119, DOI: **10.1016/j.est.2024.111119**.